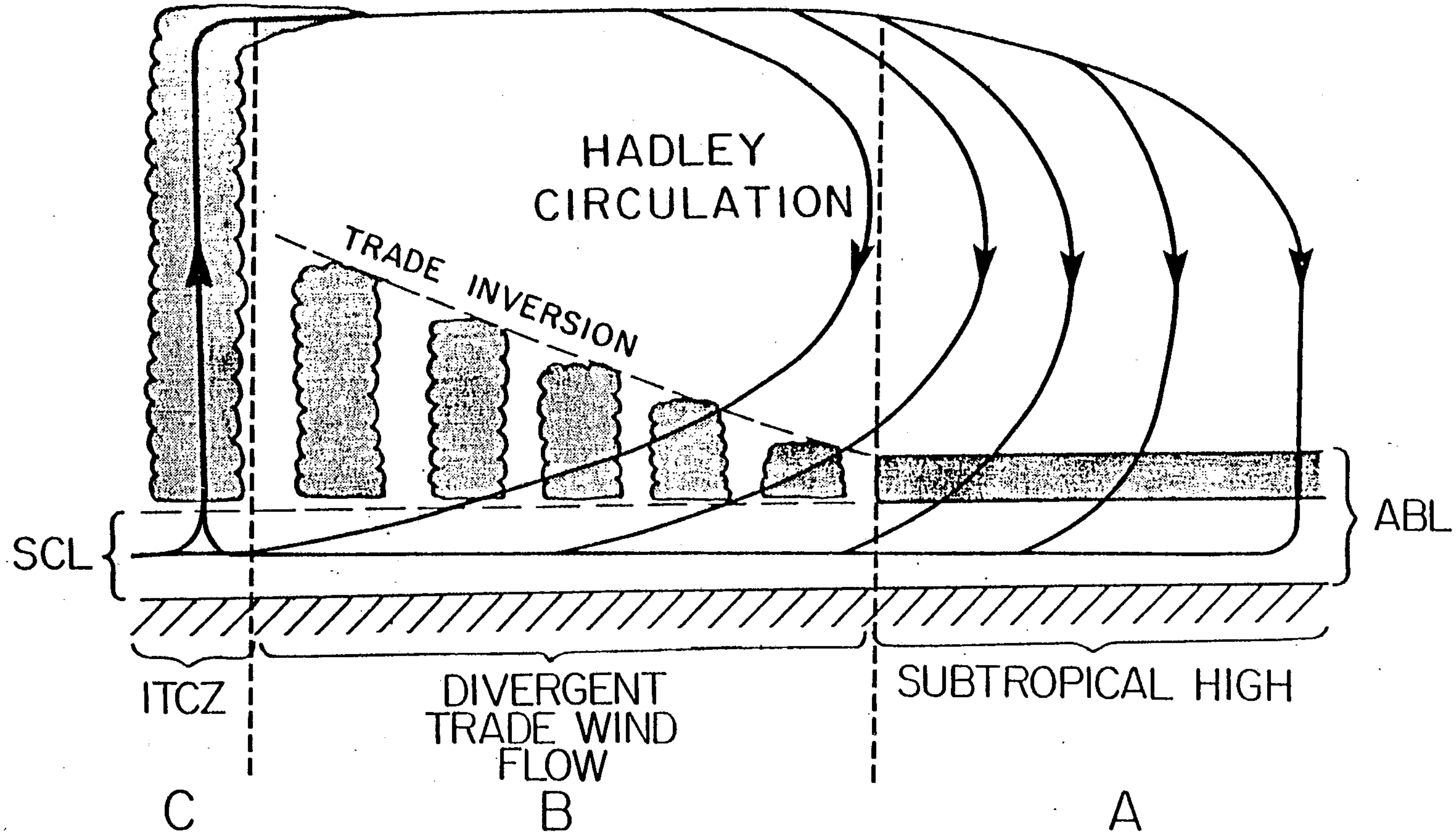
HADLEY
CIRCULATION
TRADE INVERSION
SCL
ABL
ITCZ
DIVERGENT
TRADE WIND
FLOW
SUBTROPICAL HIGH
C
B
A

Figure 2.1

Annual Stratus Cloud Amount

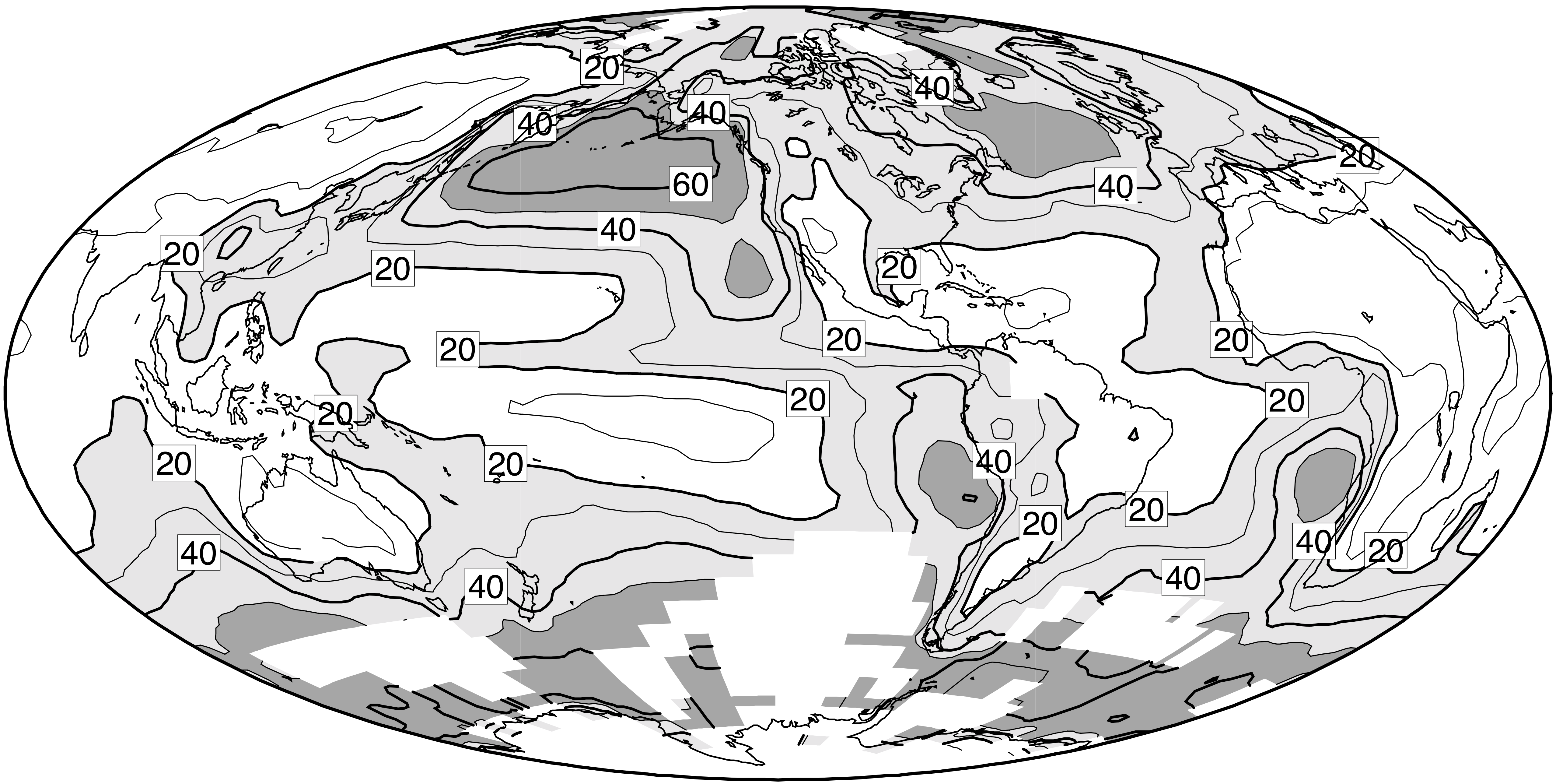

Klein and Hartmann (1993), from surface observations

Cumulus Cloud Amount

cumann.2

Klein

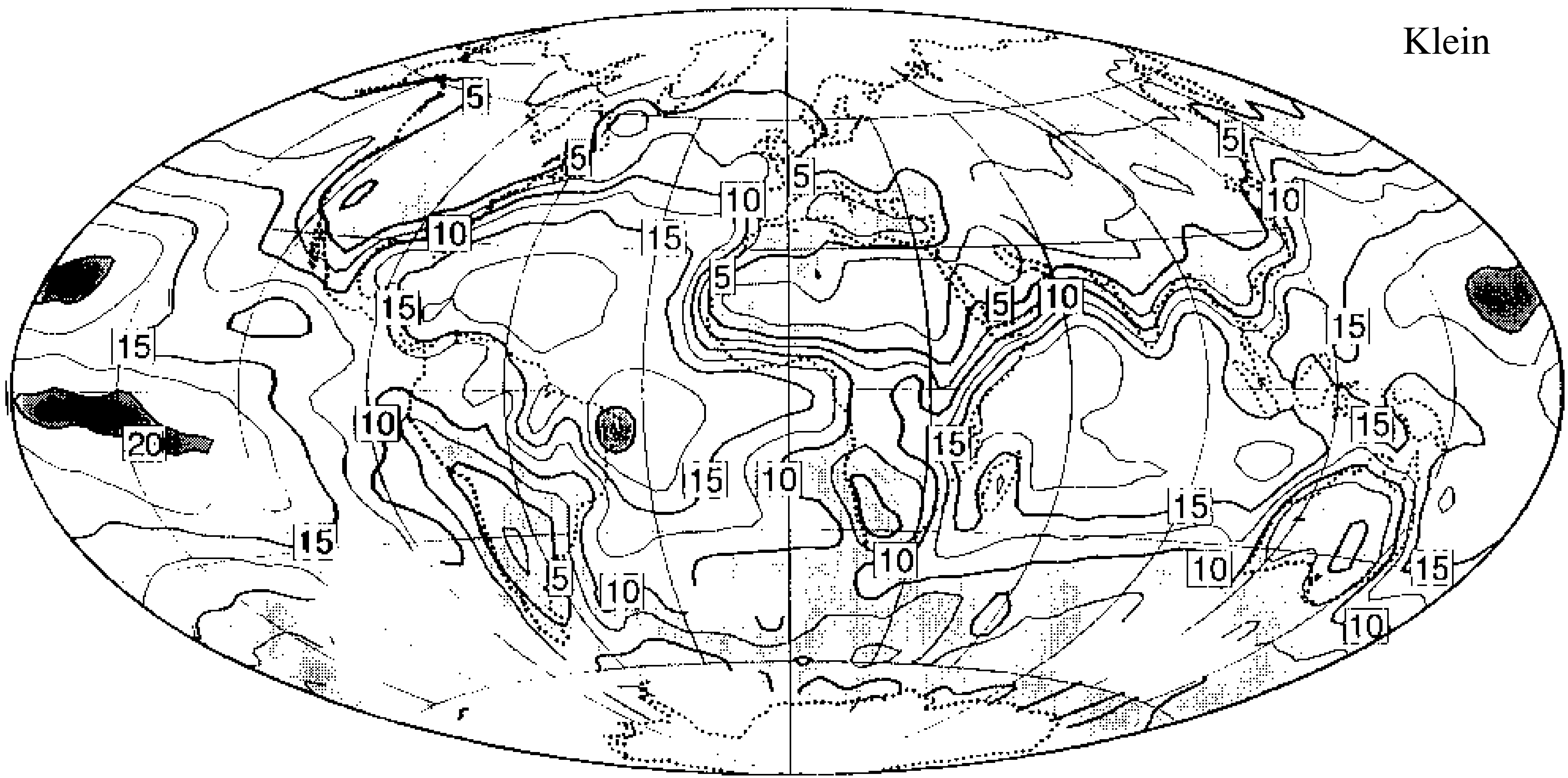

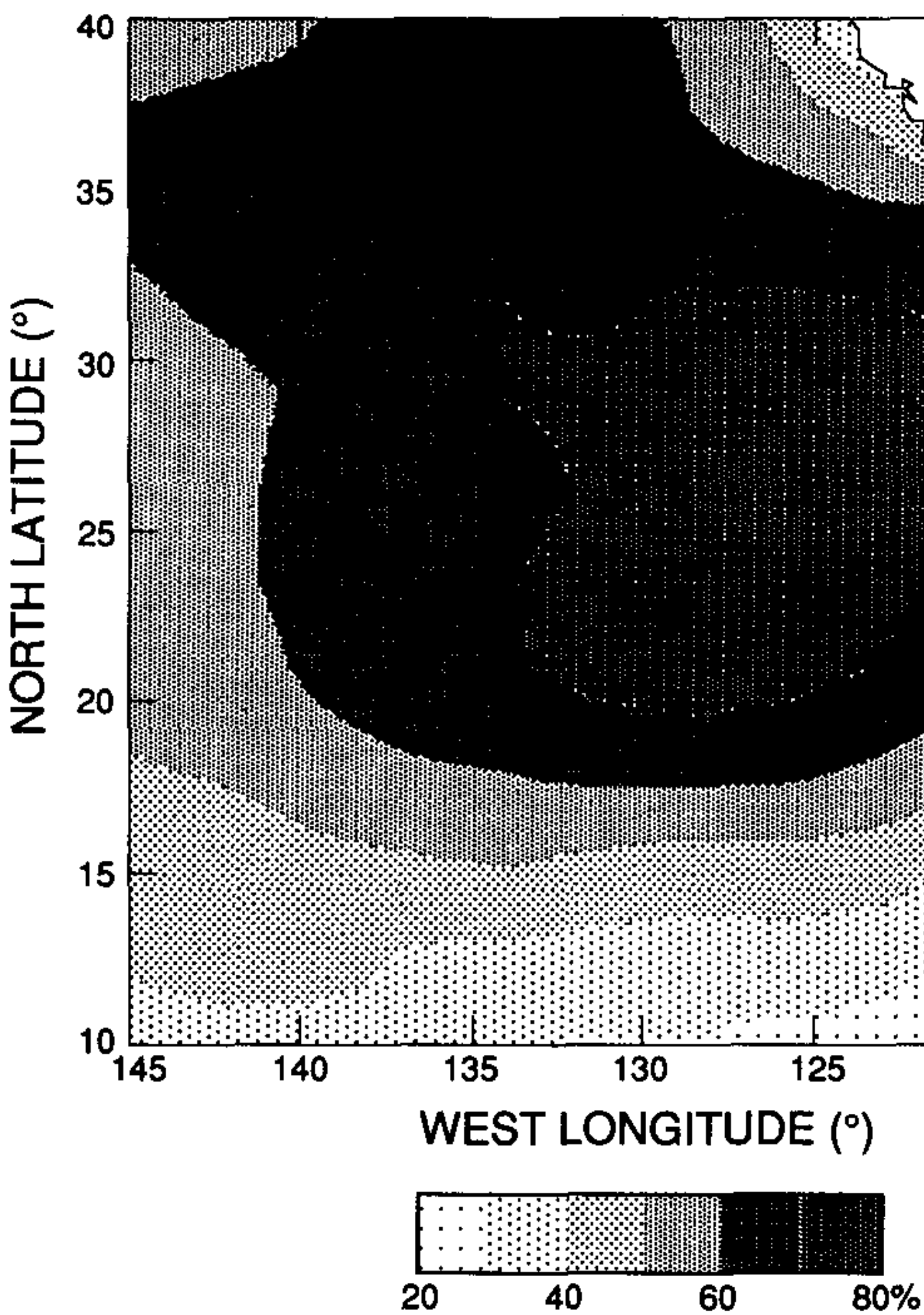

FIG. 3. Mean July low cloud cover from GOES (1983–87; from Heck et al. 1990).

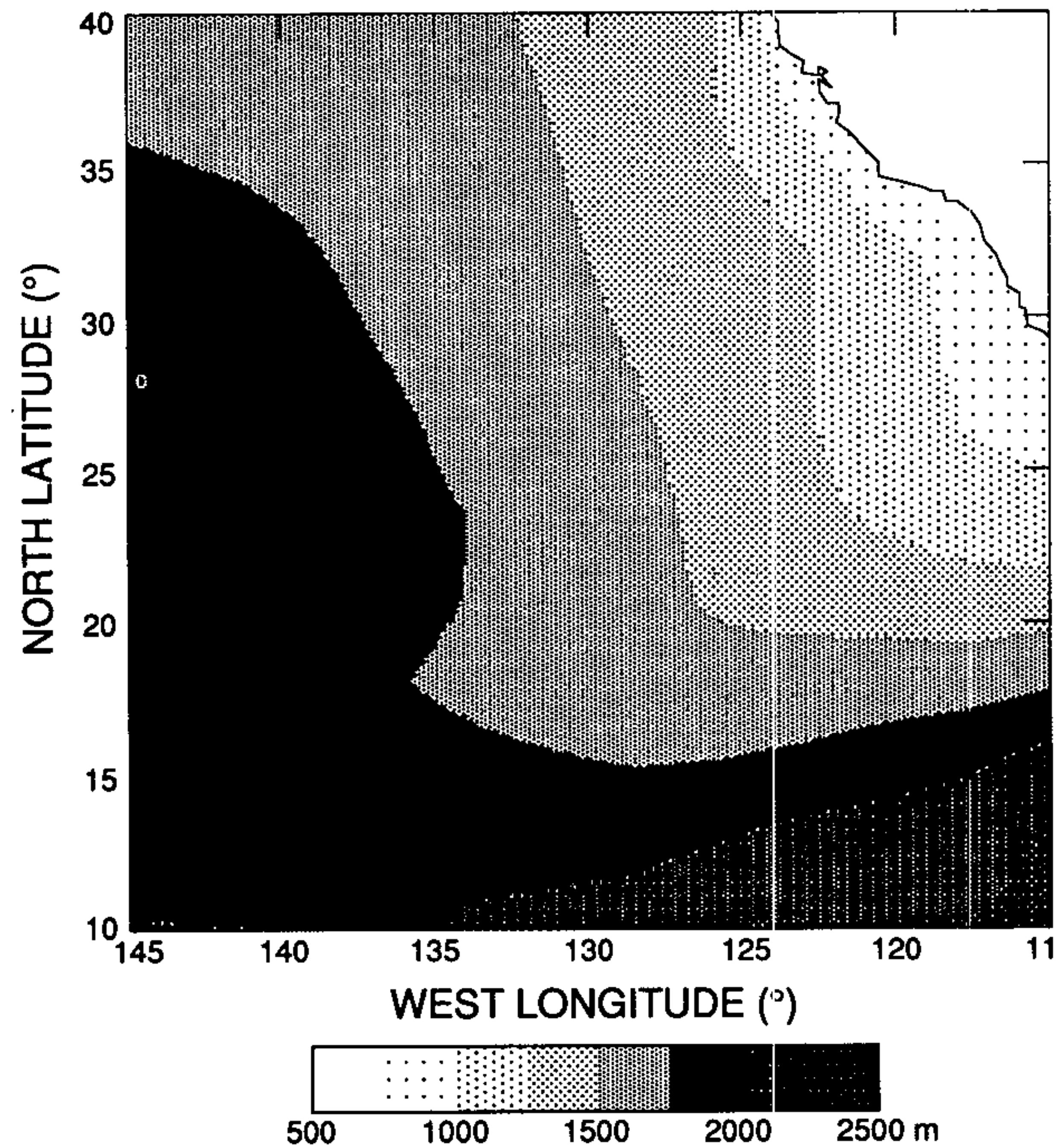

FIG. 5. Mean July low cloud-top heights from GOES (1983–87) using fixed lapse rate of 7.1 K km^{-1}.

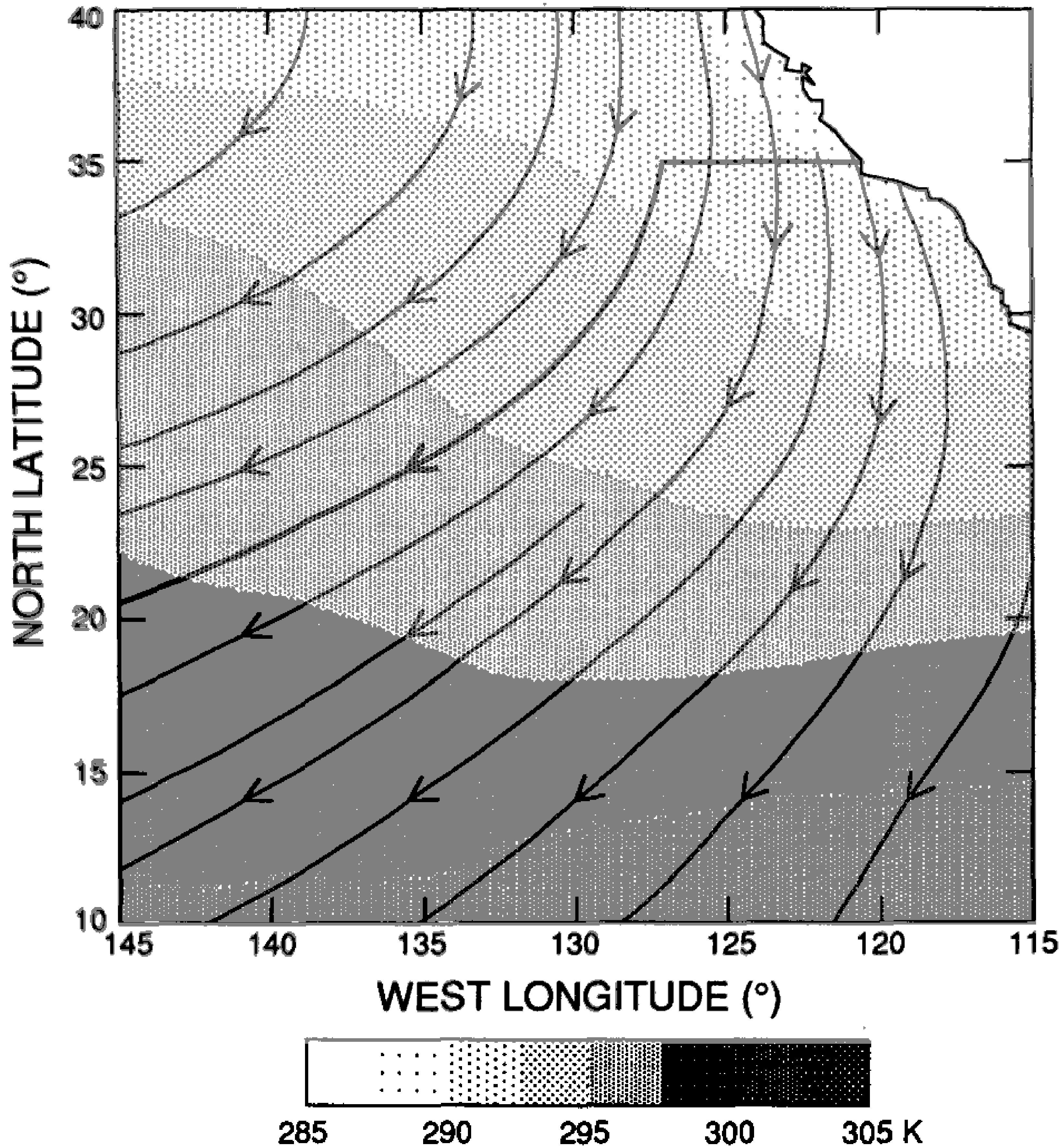
40
35
30
25
20
15
10
NORTH LATITUDE (°)
145
140
135
130
125
120
115
WEST LONGITUDE (°)
285
290
295
300
305 K

TABLE 1. Averages along mean trajectory toward increasing SST for COADS and satellite data and selected parameters derived from equilibrium CBL model.

Surface							CBL top		Satellite		Mixing-line retrieval			
SST (K)	P_O (hPa)	V_O (m s^{-1})	ω_O (Pa s^{-1})	θ_A (K)	q_A (g kg^{-1})	θ_{eA} (K)	θ_{es} (K)	q (g kg^{-1})	Cloud (%)	T_{CLD} (K)	P_T (hPa)	P_B (hPa)	Γ_{CBL} (K km^{-1})	Γ_{ML}
289.83	1017.0	7.73	.121	288.49	10.07	316.8	352.9	3.44	62.1	283.7	918.0	971.8	7.1	0.81
291.18	1018.1	7.54	.117	289.70	10.38	319.1	351.9	3.24	64.0	283.5	901.4	958.7	7.5	0.73
292.17	1018.5	7.18	.111	290.52	10.79	321.1	351.6	3.16	69.2	284.0	898.8	954.6	7.8	0.64
293.14	1017.6	6.72	.104	291.54	11.33	323.8	351.2	3.29	66.9	284.9	901.8	950.2	8.1	0.55
294.17	1017.4	6.51	.100	292.50	11.99	326.8	350.4	3.36	67.3	284.9	887.2	948.8	8.0	0.50
295.24	1016.7	6.44	.099	293.55	12.64	329.8	350.8	3.34	73.1	284.8	871.5	945.0	7.9	0.46
296.19	1015.8	6.81	.104	294.55	13.54	333.5	351.0	3.53	68.2	285.6	869.8	946.4	8.0	0.40
297.15	1015.0	6.92	.105	295.57	14.16	336.5	350.9	3.74	63.2	285.6	856.7	941.5	7.9	0.37
298.14	1014.8	7.46	.113	296.59	15.03	340.2	350.2	3.68	52.5	285.7	846.5	940.2	8.0	0.32
299.12	1013.3	7.43	.112	297.66	15.97	344.2	350.9	4.55	47.0	296.2	839.8	938.6	8.0	0.30
300.12	1012.1	7.00	.105	298.44	16.99	348.2	350.5	6.06	34.8	285.9	815.8	942.5	7.7	0.34
301.05	1011.5	5.40	.081	299.14	17.21	349.6	350.2	6.62	26.3	285.5	801.0	934.6	7.8	0.37

Numerical Simulation of the Stratus-to-Cumulus Transition in the Subtropical Marine Boundary Layer. Part I: Boundary-Layer Structure

STEVEN K. KRUEGER, GEORGE T. MCLEAN,* AND QIANG FU**

Department of Meteorology, University of Utah, Salt Lake City, Utah

(Manuscript received 13 June 1994, in final form 17 February 1995)

ABSTRACT

A stratus-to-cumulus transition (SCT) that resembles observations occurred in Lagrangian numerical simulations of the subtropical marine boundary layer over the northeastern Pacific Ocean southwest of California. The Lagrangian approach involves translating the domain along the climatological boundary-layer trajectory at a rate equal to the observed surface wind speed. The SST is increased at a corresponding rate. The simulations did not include drizzle, the diurnal cycle, divergence changes, or mesoscale circulations and thus demonstrate that these processes are not essential for an SCT.

A 2D numerical cloud model that can explicitly represent large convective eddies is used. Turbulence at scales smaller than the large eddies is parameterized using a third-moment turbulence closure. This type of model requires no cloud-regime-specific input and is computationally economical for multiday simulations.

The results suggest that there are four stages in the transition from the stratus-topped boundary layer (STBL) to the trade cumulus boundary layer (TCBL). The simulated transition involves two intermediate stages: the deep stratus-topped boundary layer (DSTBL) and the "cumulus-under-stratocumulus" boundary layer (CUSBL). The DSTBL, like the STBL, is well mixed. The CUSBL has a two-layer structure, like the TCBL, with a well-mixed subcloud layer and a stratified (partly mixed) cloud layer. The transition to a typical TCBL structure preceded the transition to a typical TCBL cloud fraction by about two days.

Sensitivity tests indicate that by using diurnally averaged solar radiation with the daytime-averaged solar zenith angle, the model is able to reproduce the diurnally averaged cloud-top height. Tests also suggest that the boundary-layer structure is sensitive to the above-inversion thermodynamic structure.

TABLE 1. Lagrangian simulations using the CEM.

Name	Description	Length	Result
SCT_1	SST increased from 290.2 to 299.2 K	5 days	Stratus-to-cumulus transition
SCT_2	SST increased from 295.6 to 301.0 K	3 days	Stratus-to-cumulus transition

SST increases 1.8 K/day for both simulations.

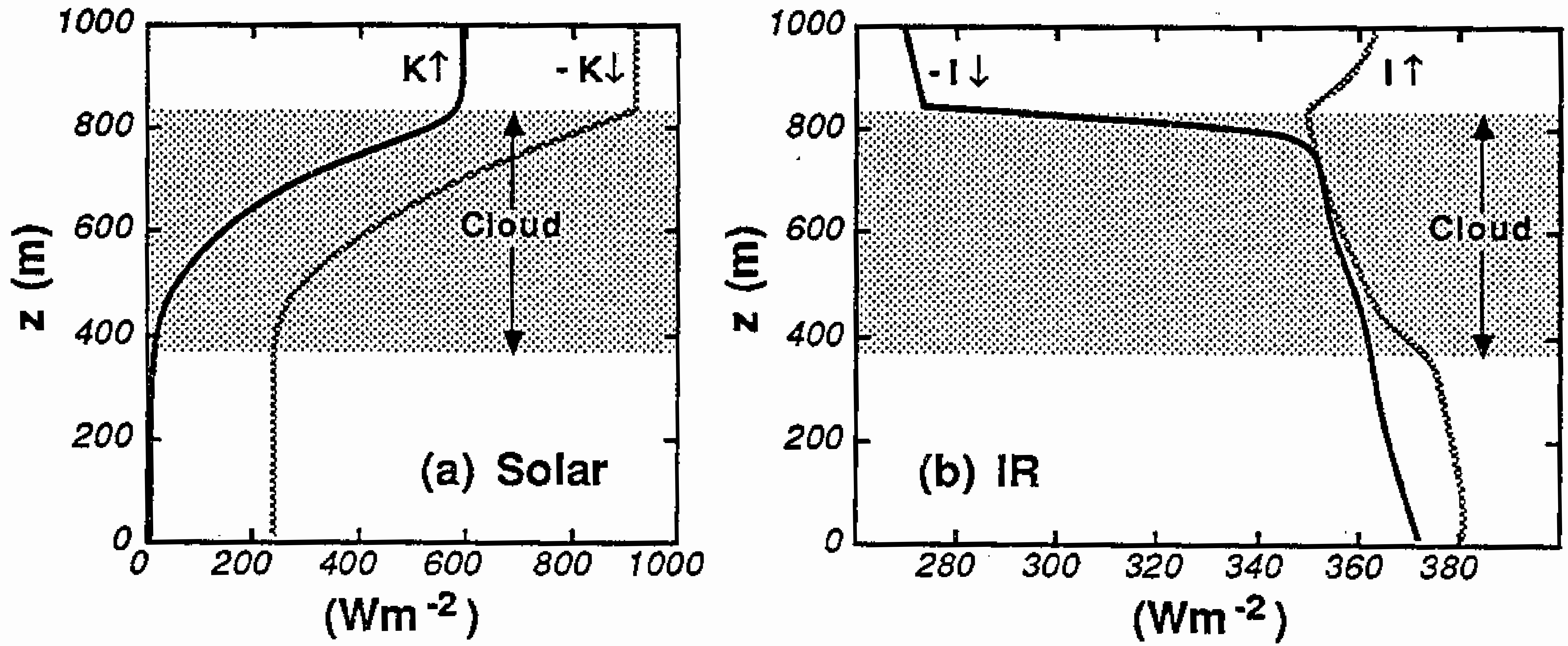

Fig. 13.4 Average (a) solar, K, and (b) IR, I, radiation fluxes. The extent of the stratocumulus cloud layer is shown by the shading. (After Nicholls, 1984).

Fig. 13.5
Profiles of net shortwave radiative flux and the corresponding heating rate in an idealized stratocumulus deck. (After Hanson, 1987).

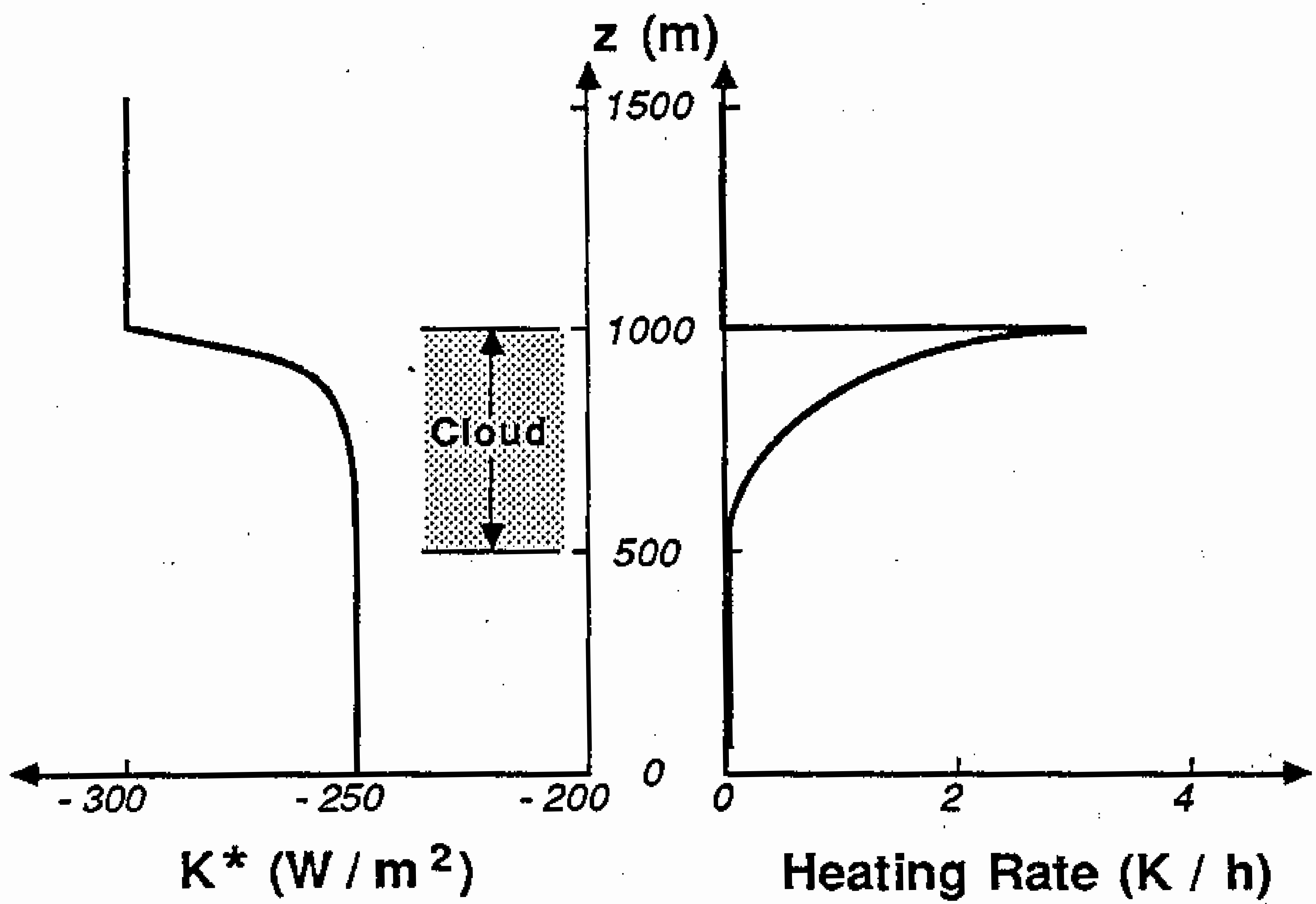

Fig. 13.7
Profiles of net longwave radiative flux and corresponding heating rate in an idealized stratocumulus deck. (After Nicholls and Leighton, 1986).

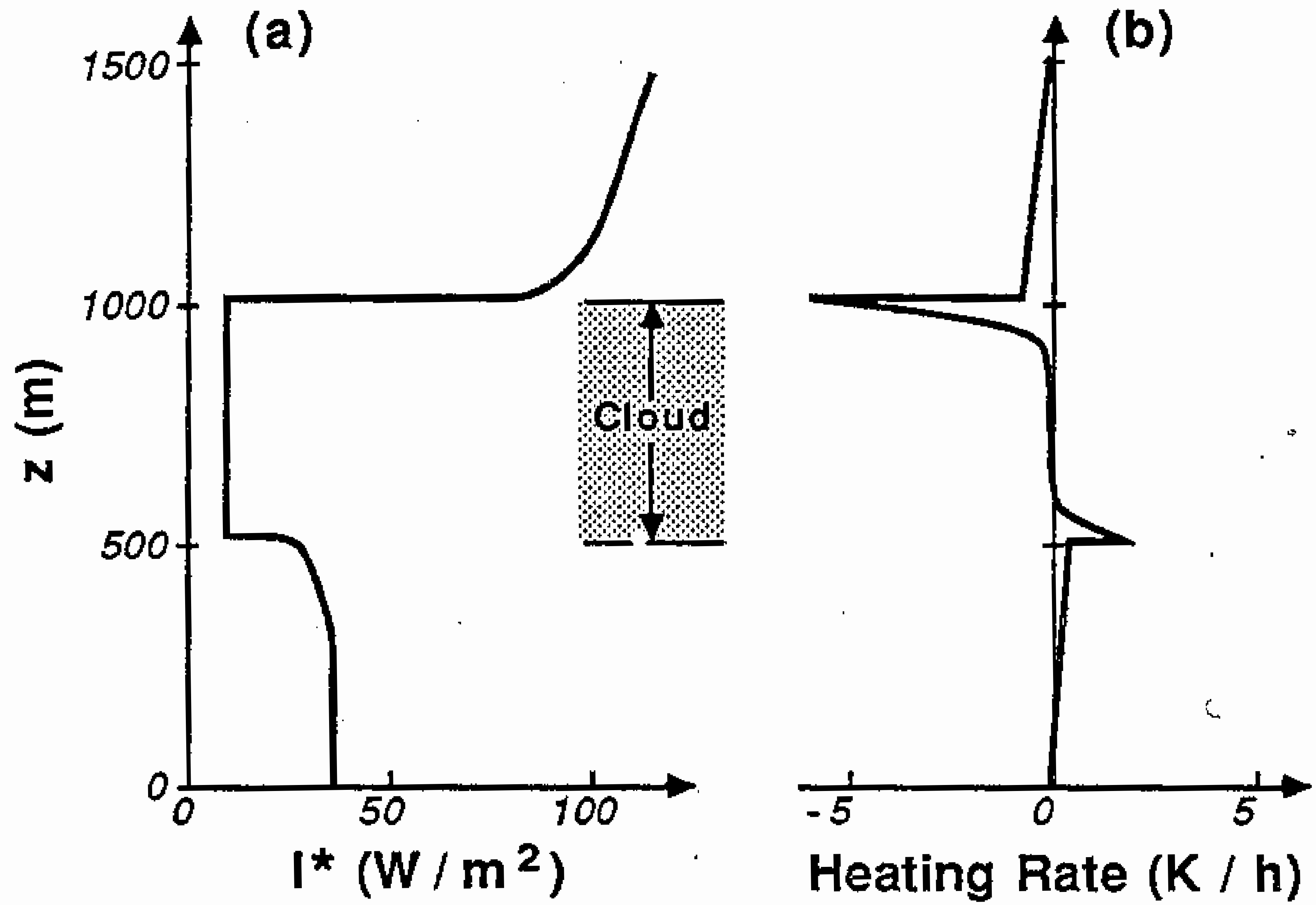

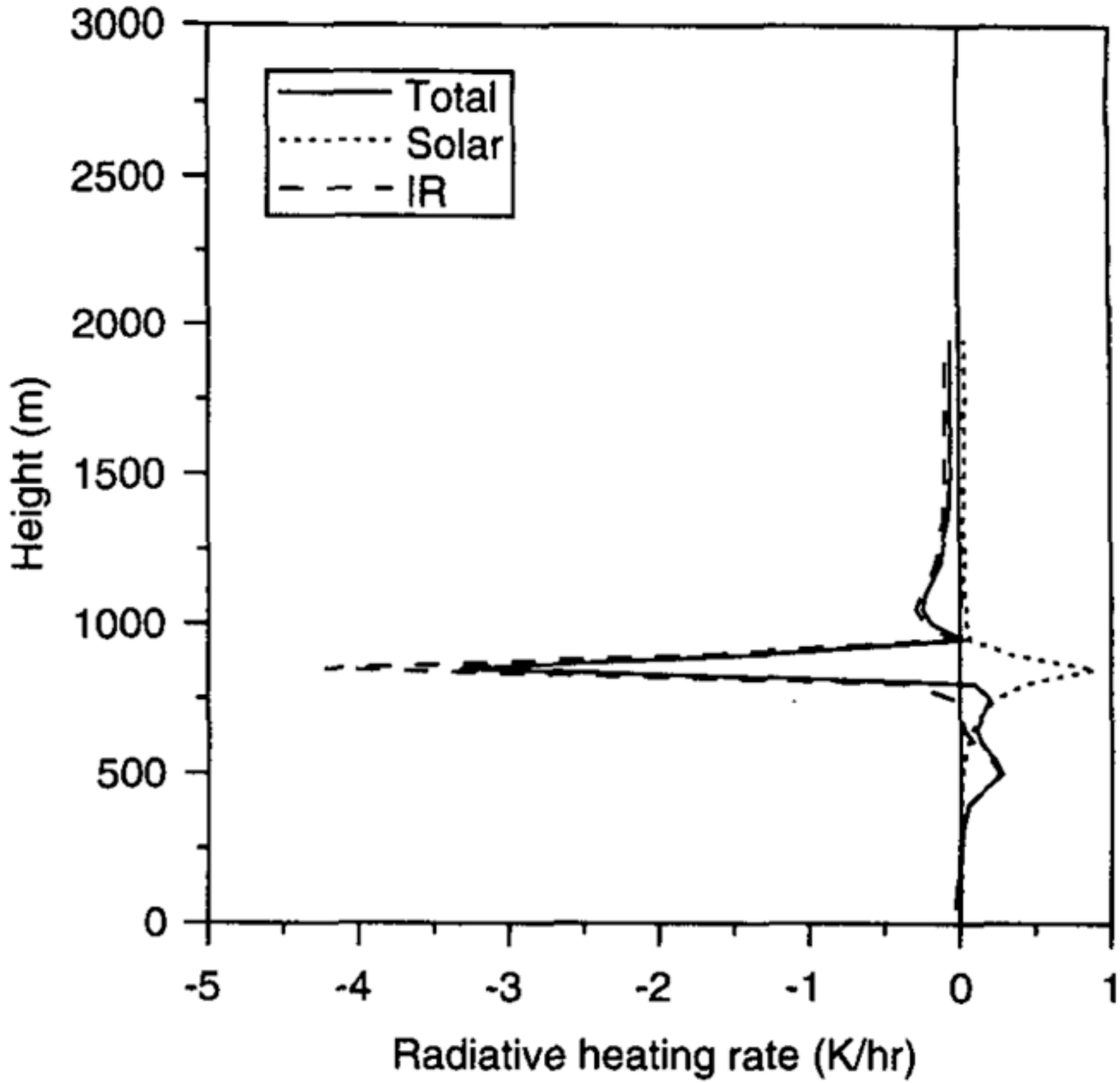

FIG. 1. Total, solar, and IR radiative-heating rates for hours 12–18 of STRATUS.

Cloud fraction vs height and time

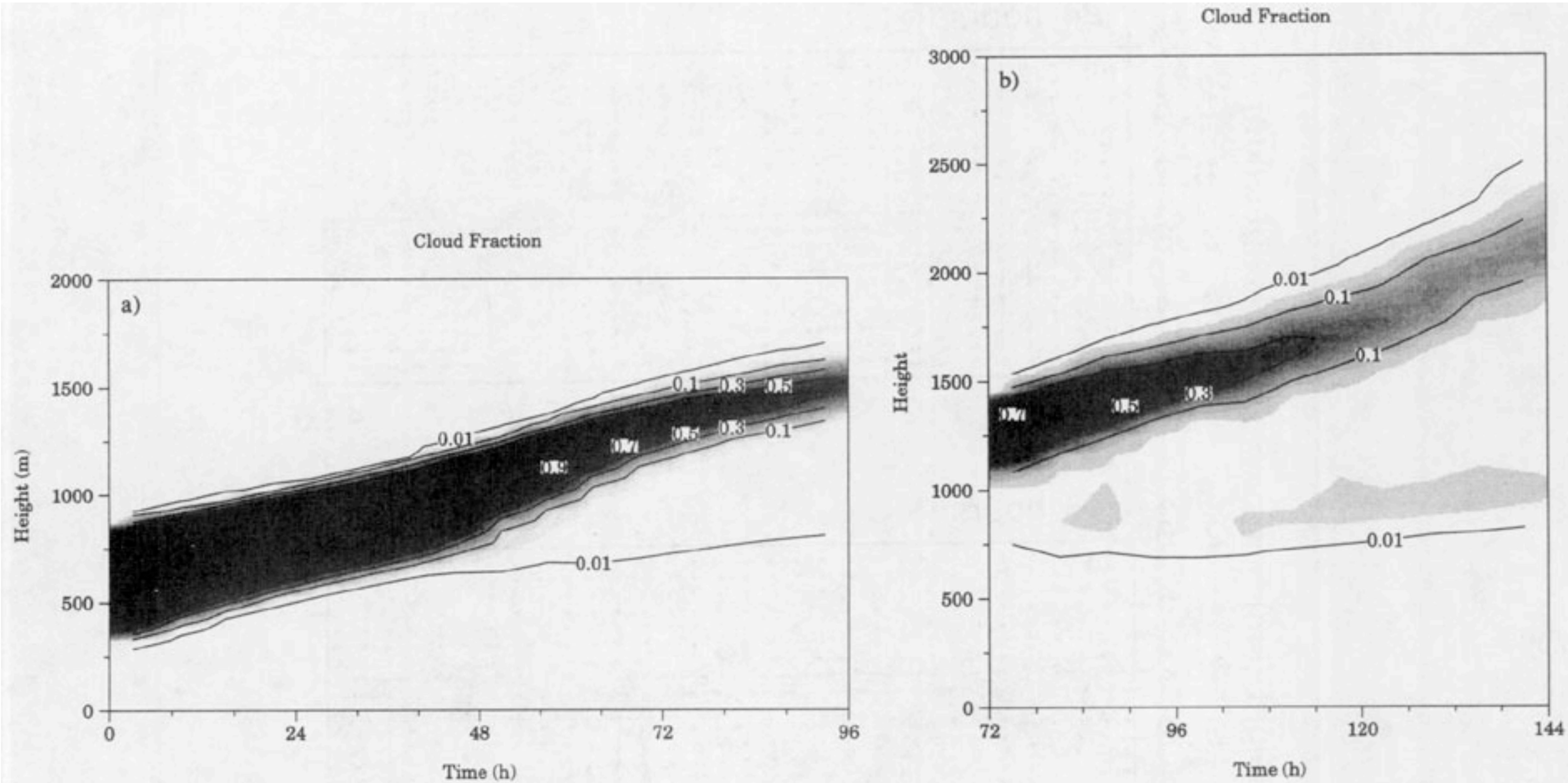

SST increases 1.8 K/day for both simulations.

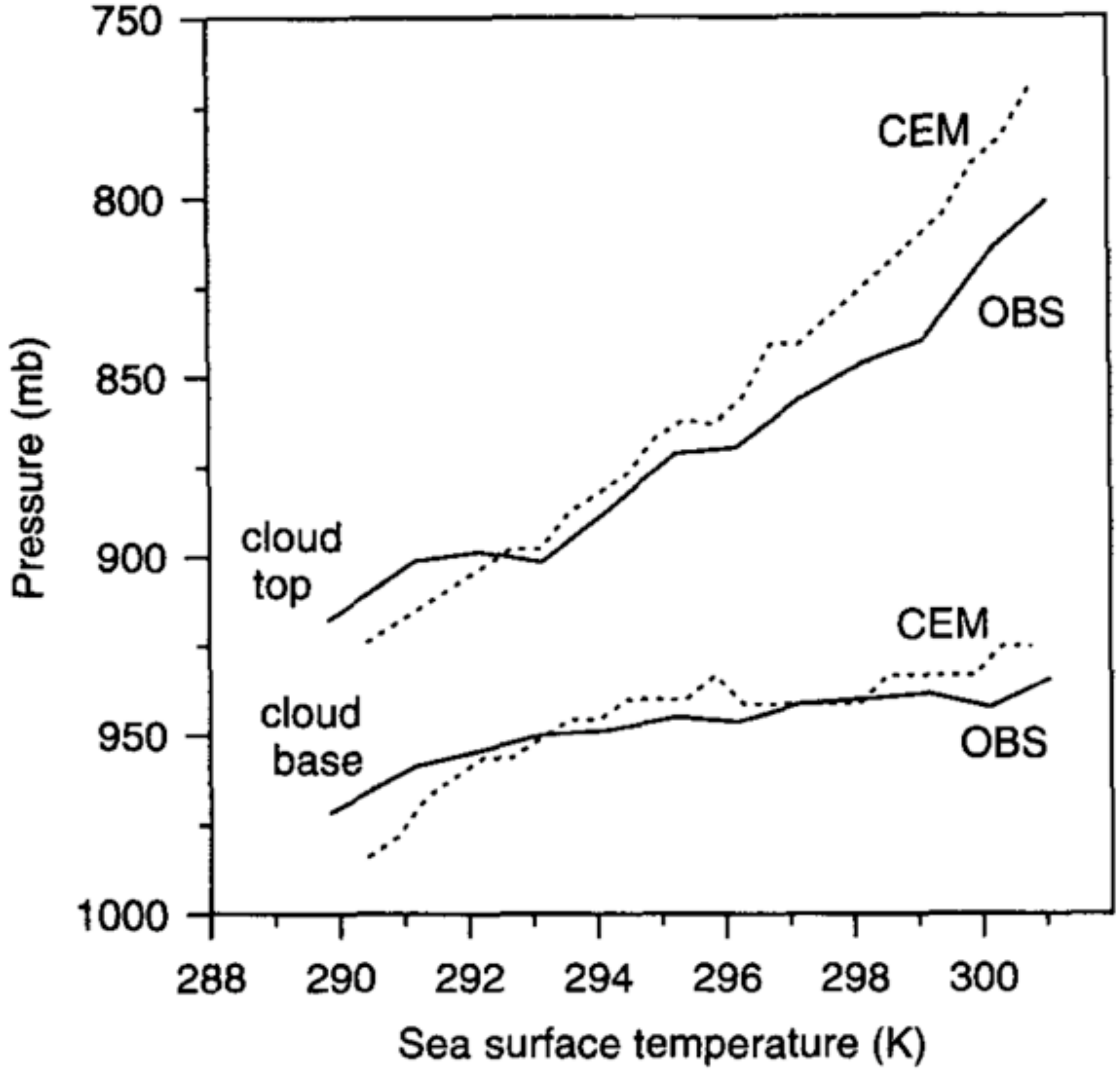

FIG. 3. Cloud-top and cloud-base pressure vs SST for the CEM (SCT_1 and SCT_2), and observations (Betts et al. 1992) along the climatological trajectory.

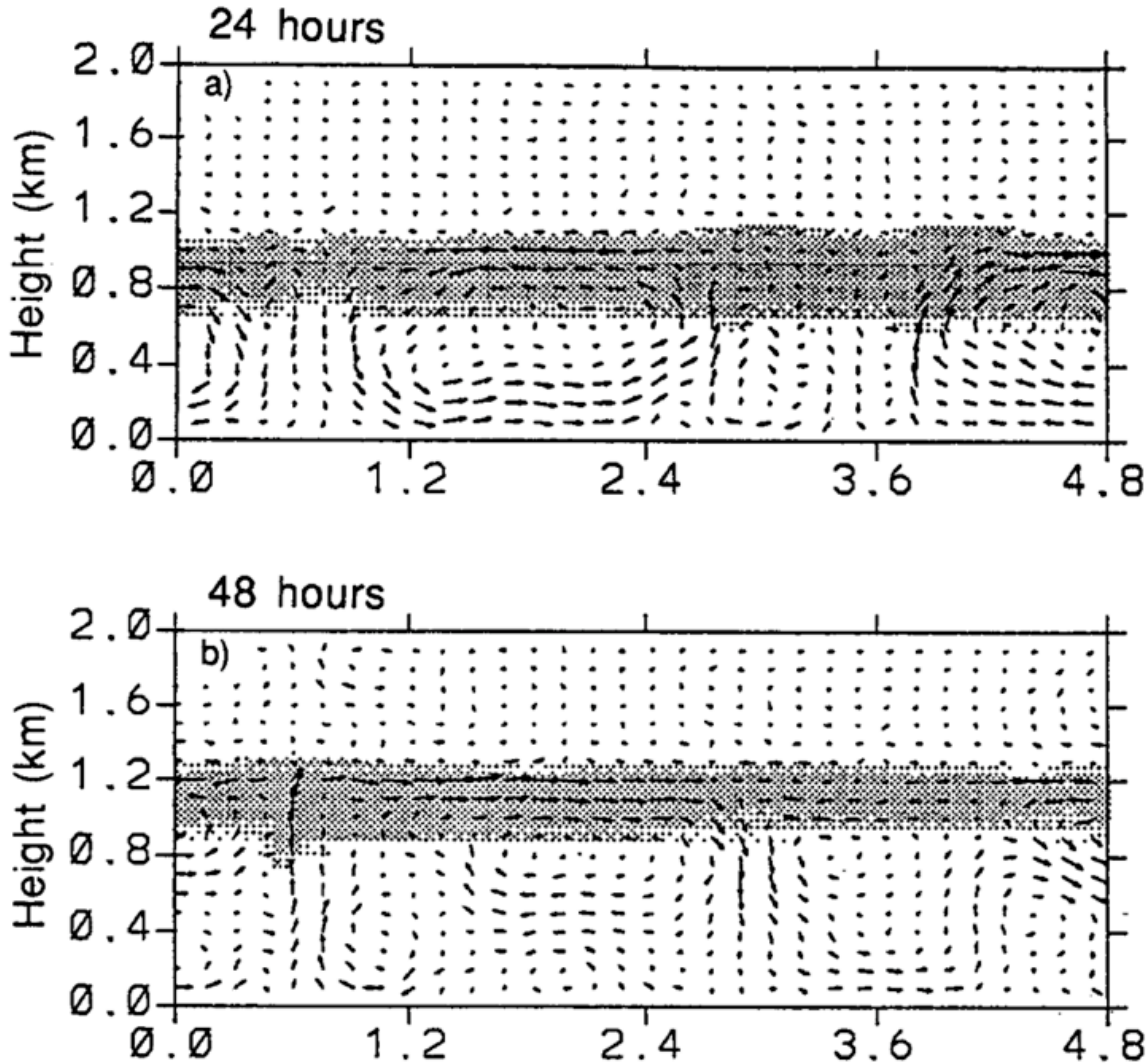

24 hours
a)
Height (km)
2.0
1.6
1.2
0.8
0.4
0.0
0.0
1.2
2.4
3.6
4.8
48 hours
b)
Height (km)
2.0
1.6
1.2
0.8
0.4
0.0
0.0
1.2
2.4
3.6
4.8

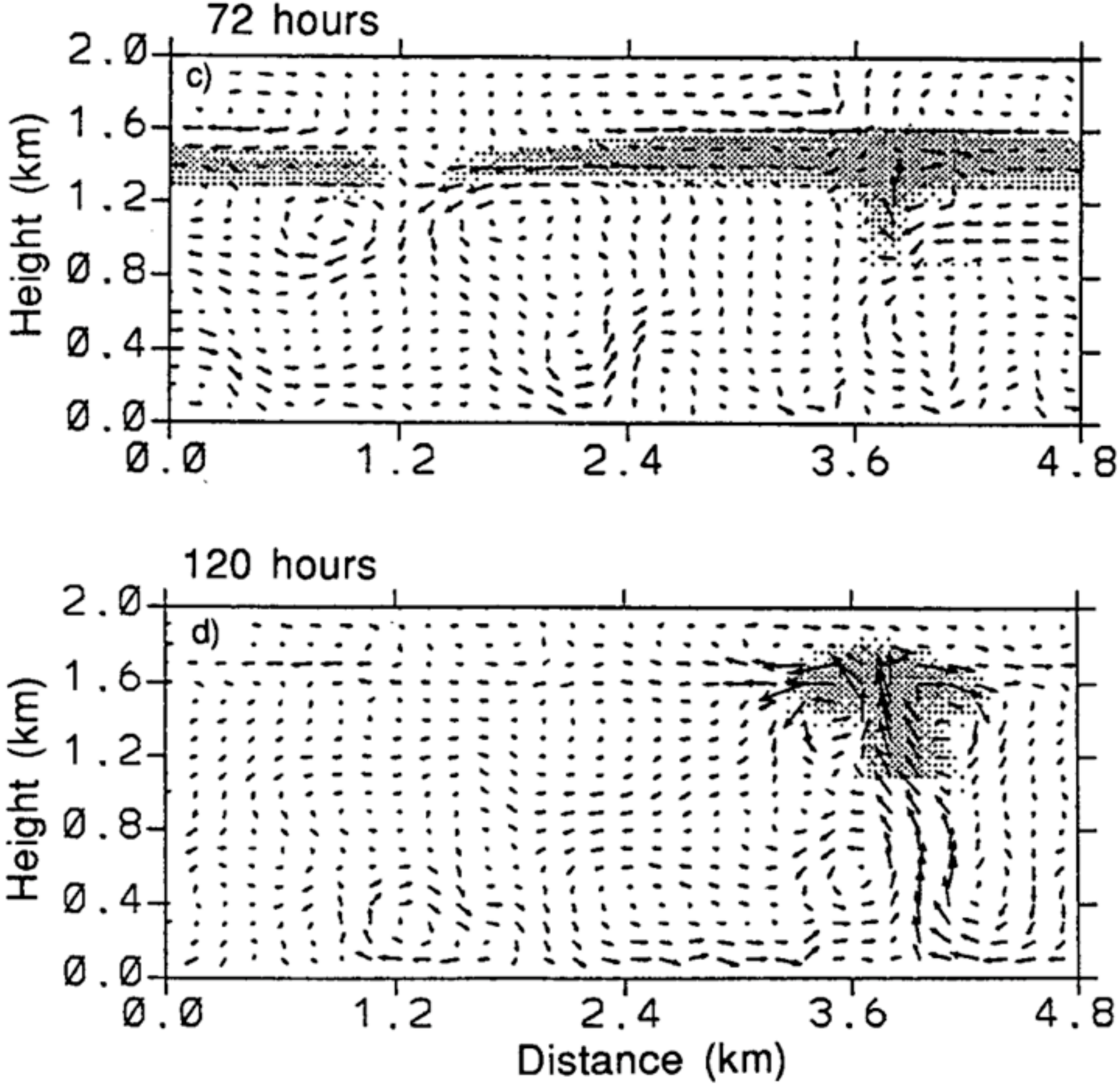

FIG. 4. Snapshots of the cloud and velocity fields at (a) 24, (b) 48, (c) 72, and (d) 120 h during SCT_1.

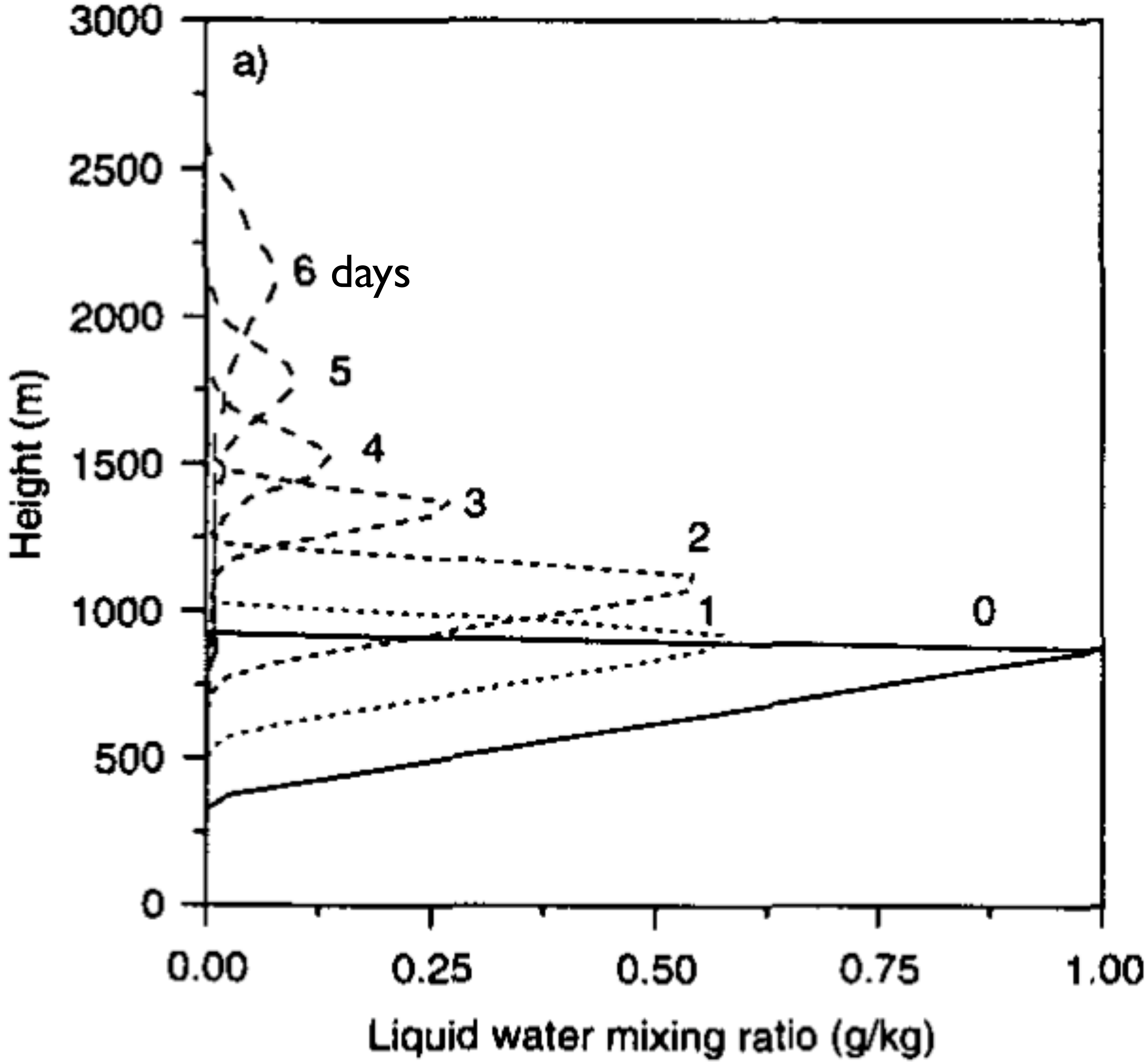
a)
6 days
5
4
3
2
1
0
Height (m)
3000
2500
2000
1500
1000
500
0
0.00
0.25
0.50
0.75
1.00
Liquid water mixing ratio (g/kg)

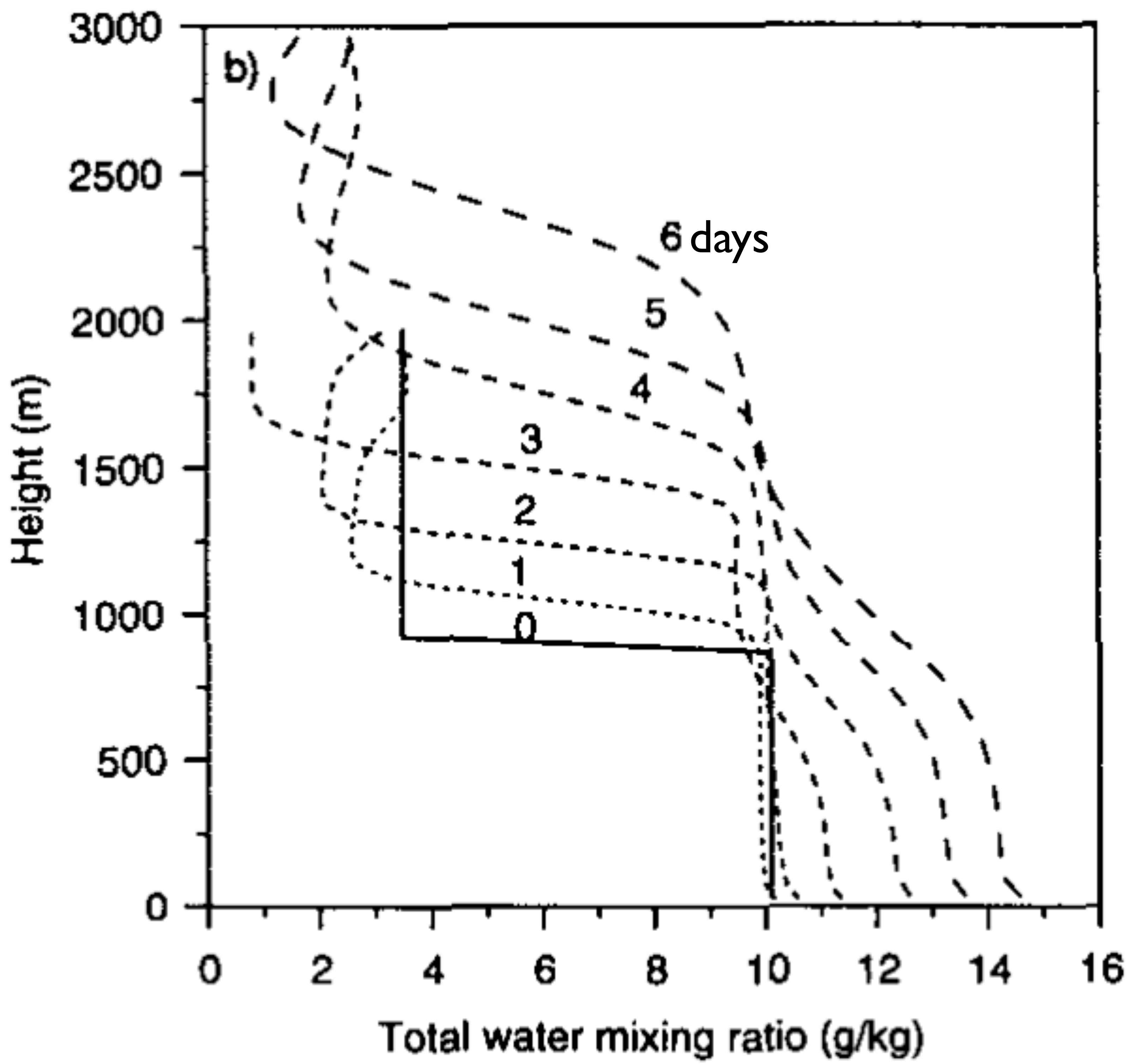

b)
6 days
5
4
3
2
1
0
Height (m)
Total water mixing ratio (g/kg)

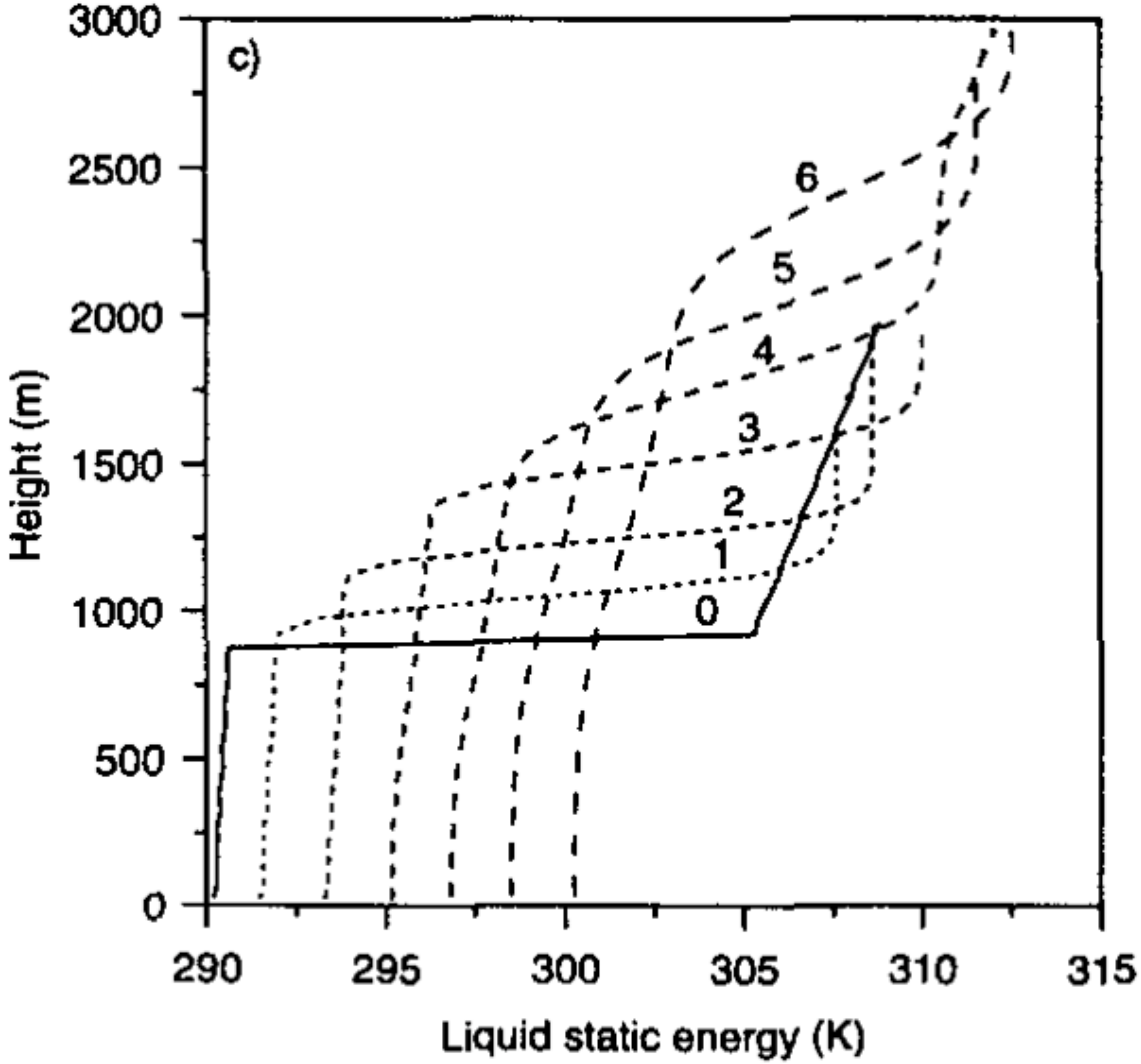

c)
Height (m)
3000
2500
2000
1500
1000
500
0
290
295
300
305
310
315
Liquid static energy (K)
0
1
2
3
4
5
6

Numerical Simulation of the Stratus-to-Cumulus Transition in the Subtropical Marine Boundary Layer. Part II: Boundary-Layer Circulation

STEVEN K. KRUEGER, GEORGE T. MCLEAN,* AND QIANG FU**

Department of Meteorology, University of Utah, Salt Lake City, Utah

(Manuscript received 13 June 1994, in final form 17 February 1995)

ABSTRACT

The progression from the stratus-topped boundary layer (STBL) to the trade cumulus boundary layer (TCBL) during a simulated stratus-to-cumulus transition (SCT) involves two intermediate stages: the deep stratus-topped boundary layer (DSTBL) and the "cumulus-under-stratocumulus" boundary layer (CUSBL). The DSTBL, like the STBL, has an active circulation that extends from the surface to the cloud top. The CUSBL, like the TCBL, has an active subcloud-layer circulation that is linked to the cloud layer by narrow cumulus updrafts. It is called a "cumulus-coupled" boundary layer.

A generally applicable convective updraft/downdraft partitioning scheme based on trajectory analysis was developed and used to analyze the boundary-layer circulation changes during the simulated SCT. The circulation analysis revealed that as the SST increased and the boundary layer changed from an STBL to a TCBL the updraft fraction in the cloud layer decreased, the convective updrafts strengthened, and the convective downdrafts weakened. The convective mass flux in the cloud layer decreased significantly as SST increased, while in the subcloud layer it changed little. The differences between updraft and downdraft properties and cloud-base levels gradually increased as SST increased.

An analysis of the vertical acceleration components of the convective updrafts and downdrafts suggests that there are three steps in the transition from an STBL circulation to a TCBL circulation. First, the STBL deepens due to increased surface buoyancy fluxes as it moves over increasing SST but remains well mixed. Next, the DSTBL gradually changes into the two-layer CUSBL. During this step, negative buoyancy in downdrafts originating near cloud top becomes less important, while positive buoyancy in (cumulus) updrafts becomes more important. This indicates that cloud-top entrainment instability does not play a significant role in the SCT. Finally, the overlying stratocumulus deck gradually dissipates and only the underlying cumulus clouds of a typical TCBL remain. This general sequence of events is supported by recent observational evidence.

TABLE 1. Simulations using the CEM.

Name	Type	Length	Result
SCT_1	Lagrangian simulation with SST increasing from 290.2 to 299.2 K	5 days	Stratus-to-cumulus transition
STRATUS	SST = 290 K	3 days	Steady STBL
TRADE_CU	SST = 301 K	12 h	Steady TCBL

TABLE 2. Simulations and time periods used to represent the four stages during the stratus-to-cumulus transition in the boundary layer (BL).

Stage	Abbreviation	Simulation	Time period	Cloud cover
Steady stratus-topped BL	STBL	STRATUS	12–18 h	1.00
Deep stratus-topped BL	DSTBL	SCT_1	42–48 h	0.99
Cu-under-Sc BL	CUSBL	SCT_1	66–72 h	0.83
Steady trade Cu BL	TCBL	TRADE_CU	6–12 h	0.03

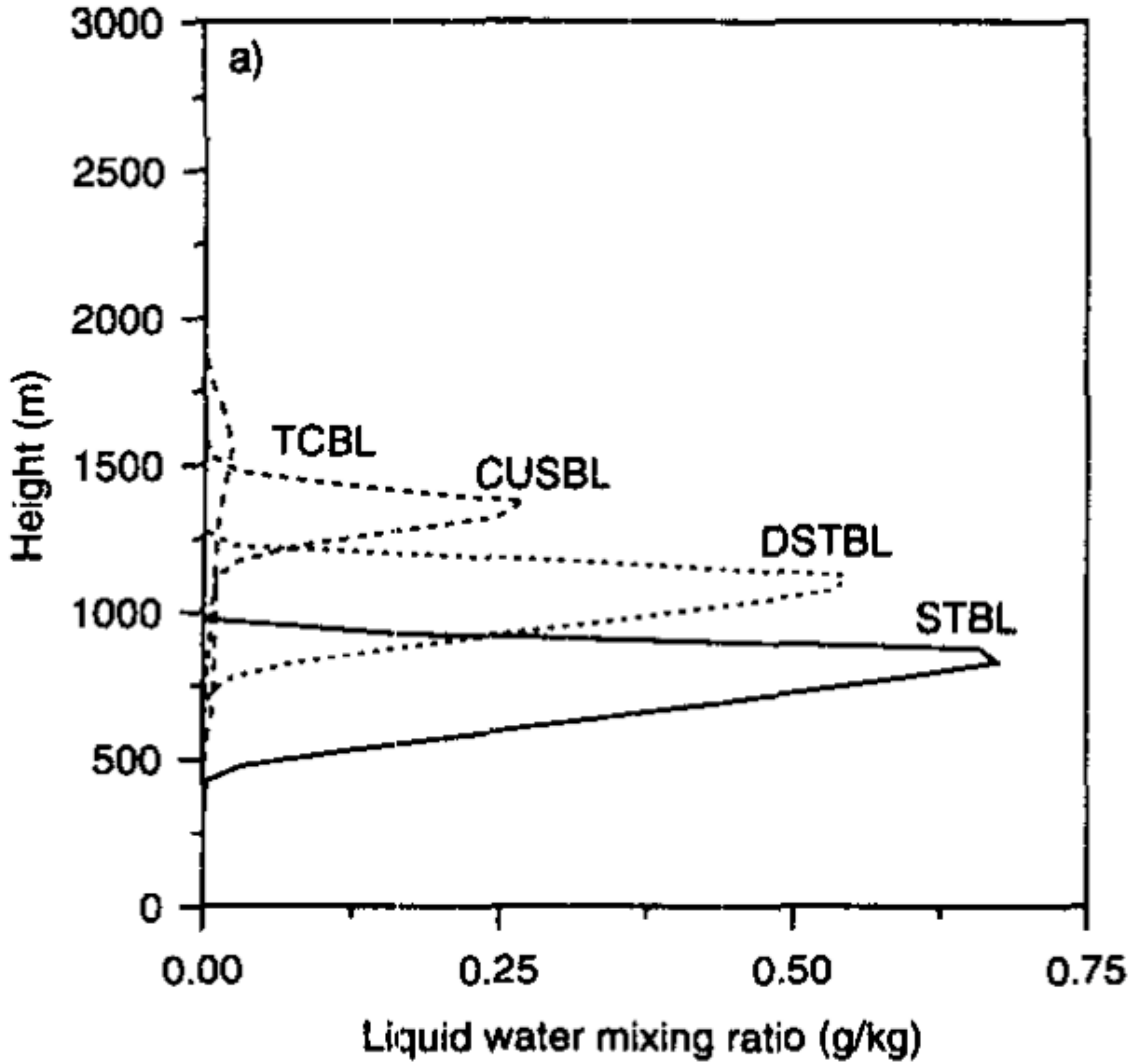

a)
3000
2500
2000
1500
1000
500
0
Height (m)
TCBL
CUSBL
DSTBL
STBL
0.00
0.25
0.50
0.75
Liquid water mixing ratio (g/kg)

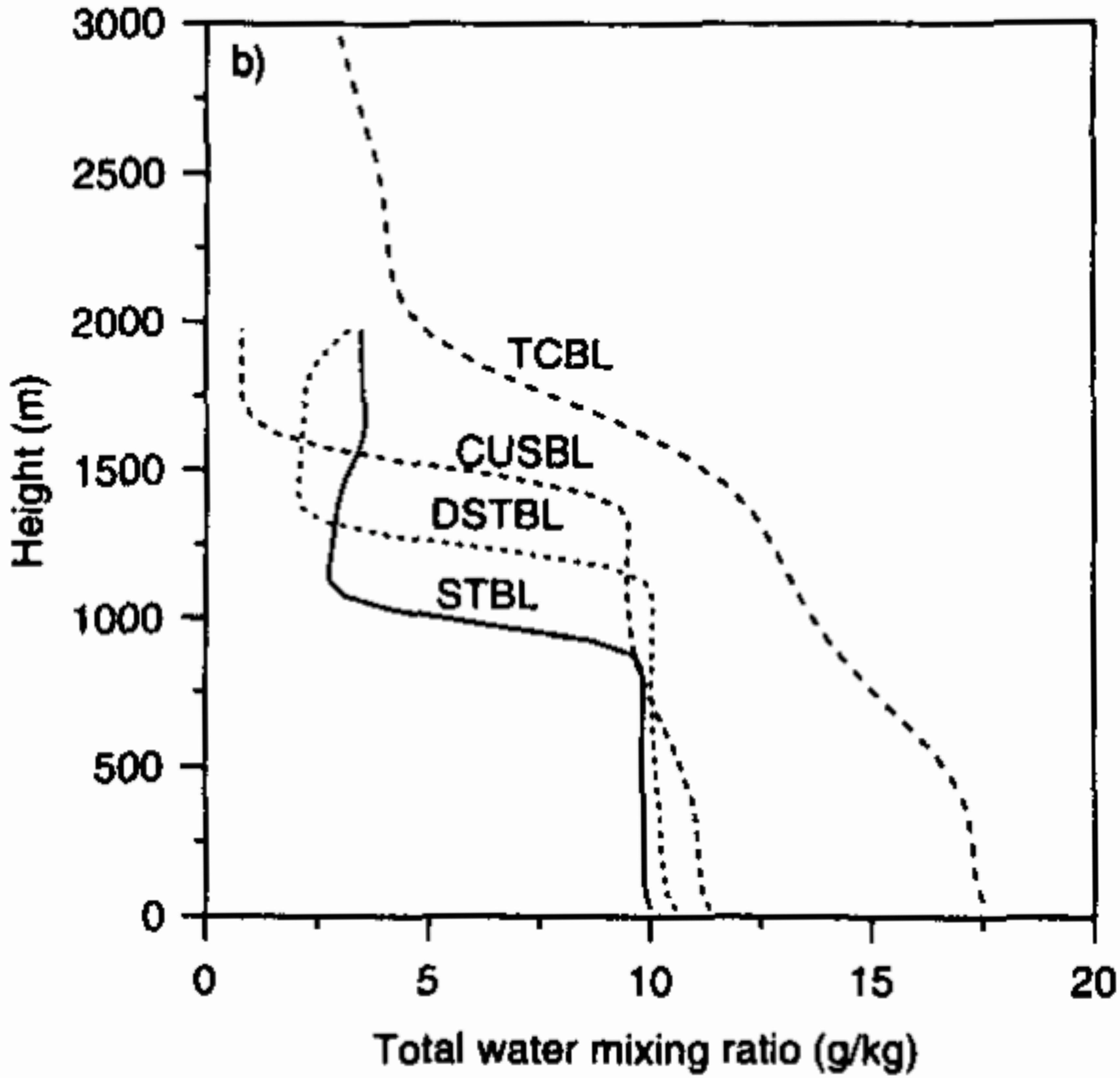
b)
TCBL
CUSBL
DSTBL
STBL
Height (m)
Total water mixing ratio (g/kg)
0
500
1000
1500
2000
2500
3000
0
5
10
15
20

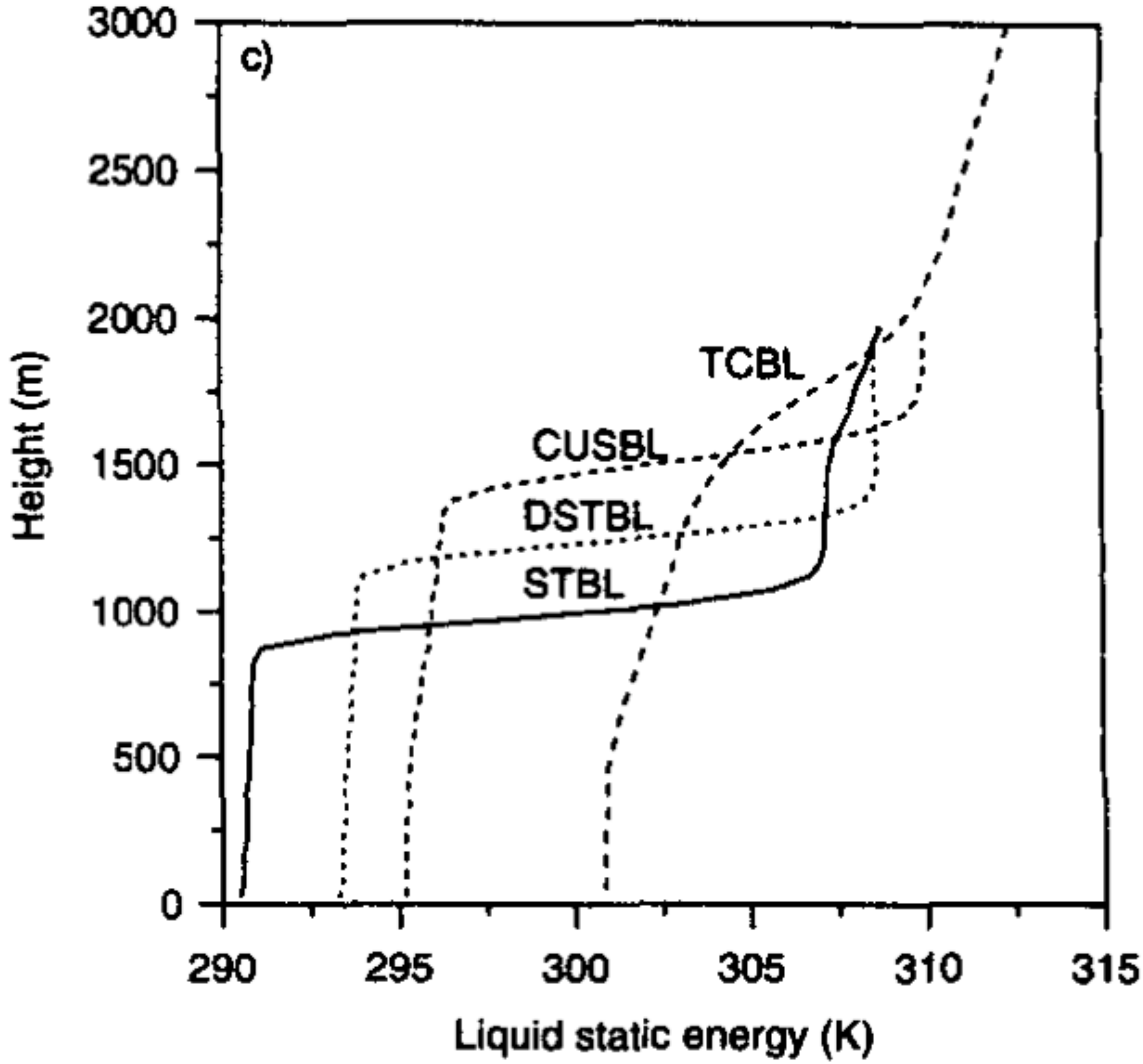
c)
3000
2500
2000
1500
1000
500
0
Height (m)
290
295
300
305
310
315
Liquid static energy (K)
TCBL
CUSBL
DSTBL
STBL

The Convective Mass Flux Model

σ: updraft fraction

$$\bar{\psi} = \sigma\psi_u + (1-\sigma)\psi_d$$

The convective flux F_ψ is

$$F_\psi = \rho\overline{w'\psi'} = M_c(\psi_u - \psi_d)$$

where

$$\begin{aligned} M_c &\equiv \rho\sigma(1-\sigma)(w_u - w_d) \\ &= \rho\sigma(w_u - \bar{w}) \\ &\approx \rho\sigma w_u \end{aligned}$$

Mixed Layer Model:
$M_c \to \infty$,
$\psi_u - \psi_d \to 0$

More general bulk models predict M_c, σ, ψ_u, ψ_d.

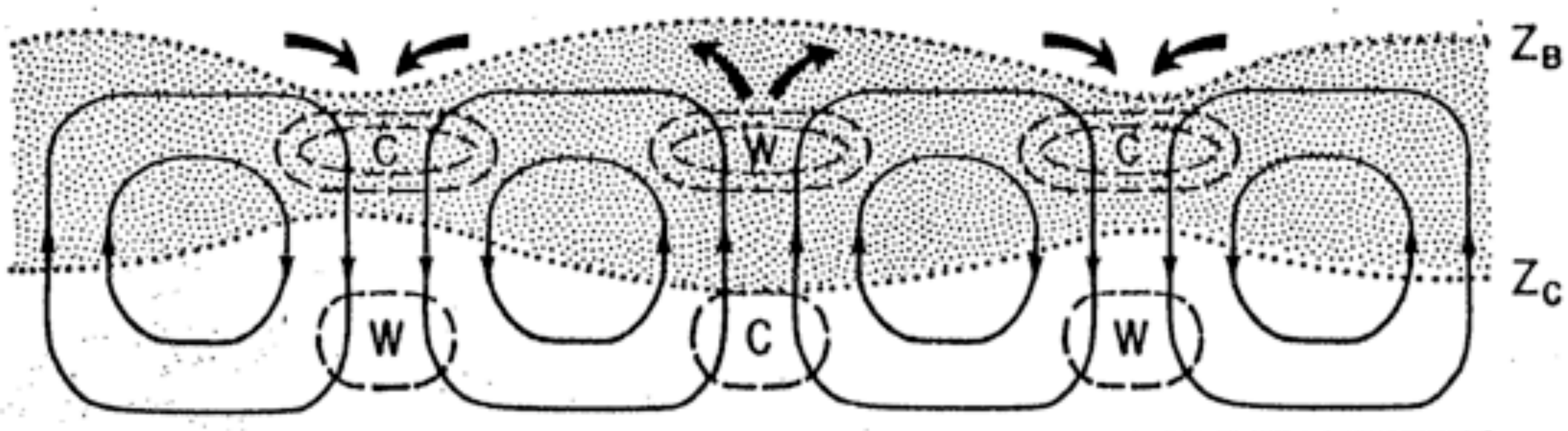

Schubert et al. 1979

Convective Mass Flux Analysis

- Identify *convective* updrafts and downdrafts using three partitioning methods:
  - ***Velocity sorting:*** Use local vertical velocity. (OK if gravity waves are absent.)
  - ***Cloud fraction sorting:*** Use local cloud fraction. (OK when updrafts are cloudy, downdrafts are clear.)
  - ***Lagrangian sorting:*** Separate parcel trajectories into convective updraft and downdraft segments. (Generally OK.)

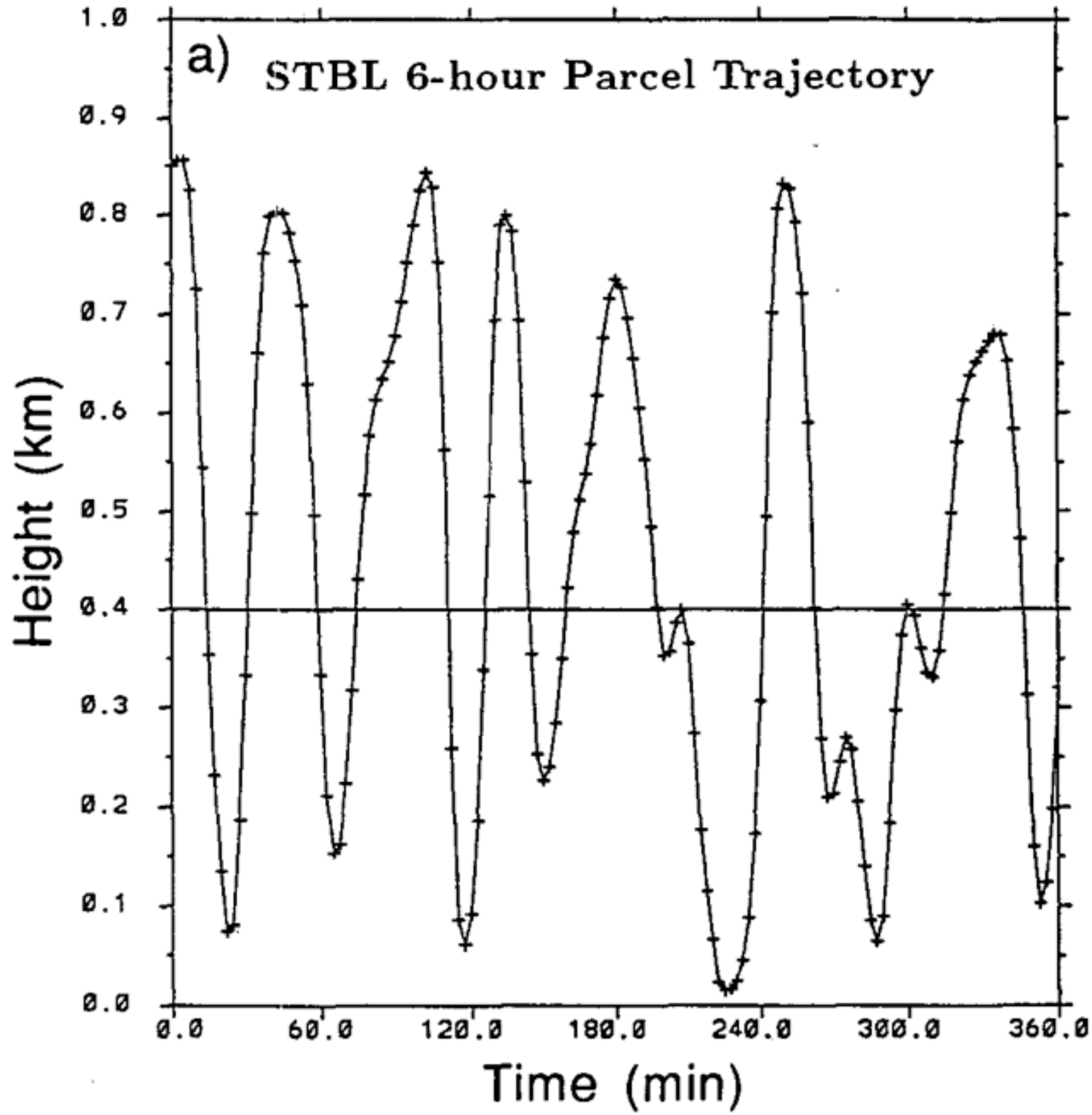
a)
STBL 6-hour Parcel Trajectory
Height (km)
Time (min)
1.0
0.9
0.8
0.7
0.6
0.5
0.4
0.3
0.2
0.1
0.0
0.0
60.0
120.0
180.0
240.0
300.0
360.0

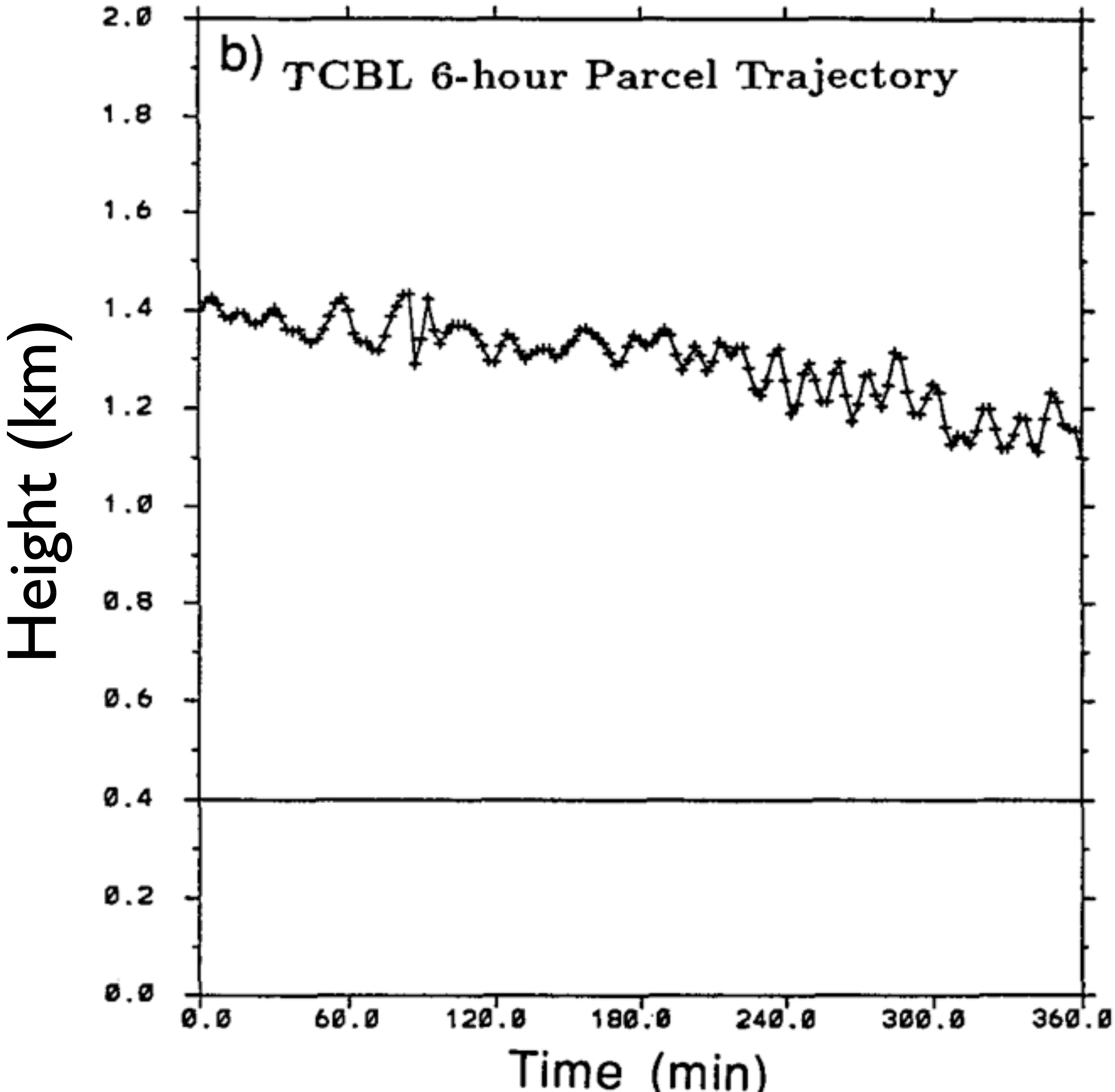
b) TCBL 6-hour Parcel Trajectory
Height (km)
2.0
1.8
1.6
1.4
1.2
1.0
0.8
0.6
0.4
0.2
0.0
0.0
60.0
120.0
180.0
240.0
300.0
360.0
Time (min)

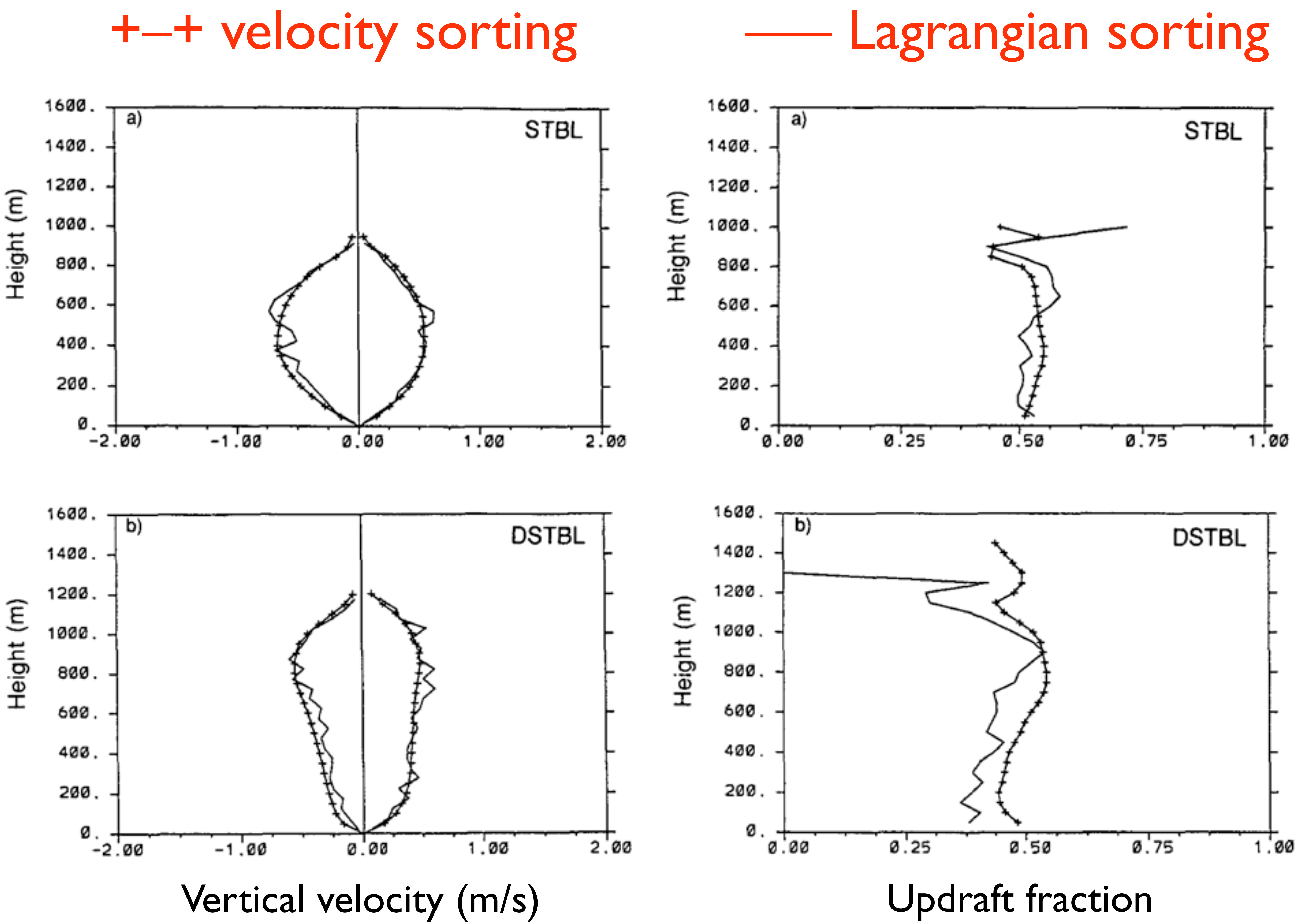

+–+ velocity sorting
—— Lagrangian sorting
a)
STBL
Height (m)
1600.
1400.
1200.
1000.
800.
600.
400.
200.
0.
-2.00
-1.00
0.00
1.00
2.00
0.00
0.25
0.50
0.75
1.00
b)
DSTBL
Vertical velocity (m/s)
Updraft fraction

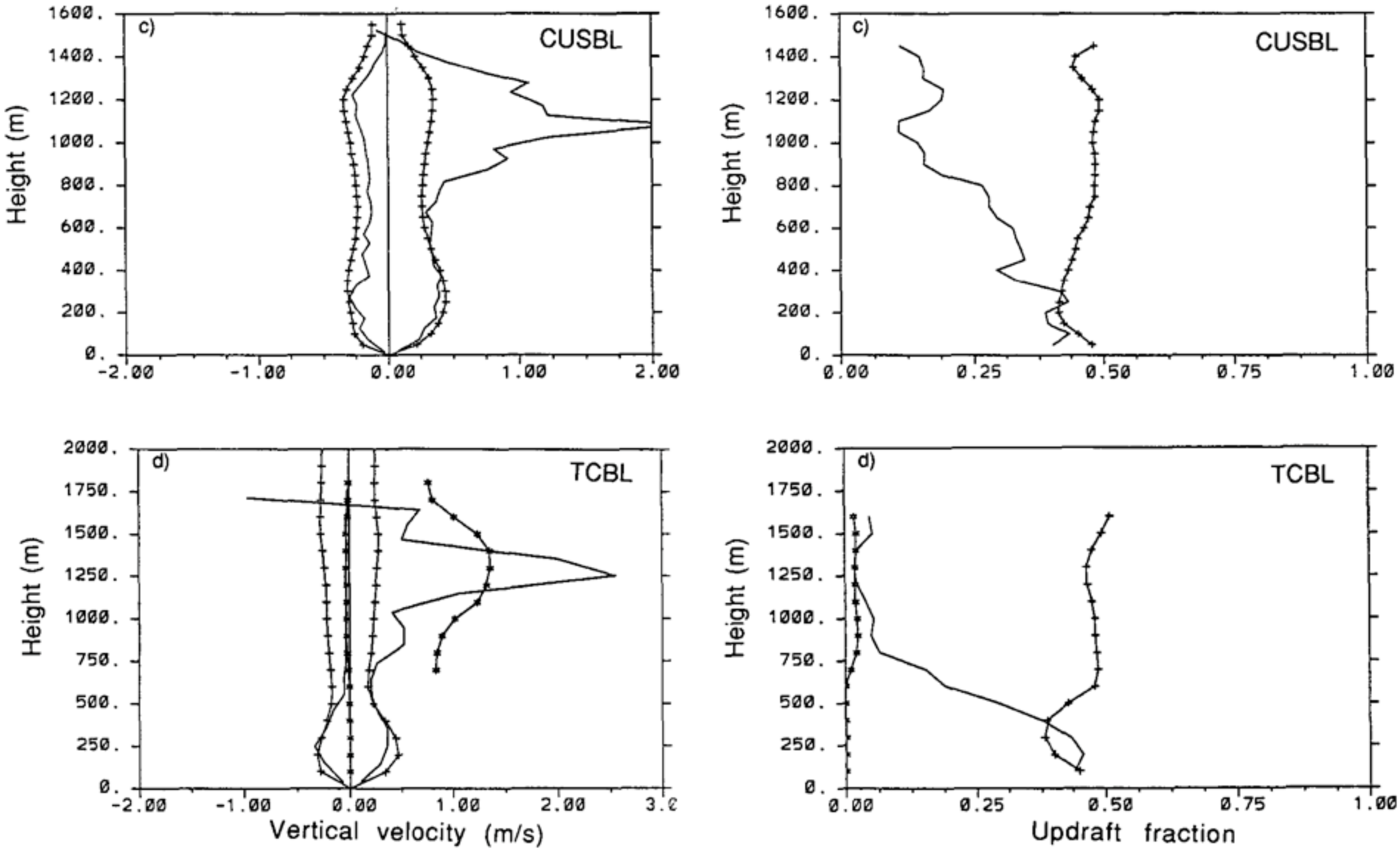

* cloud fraction sorting

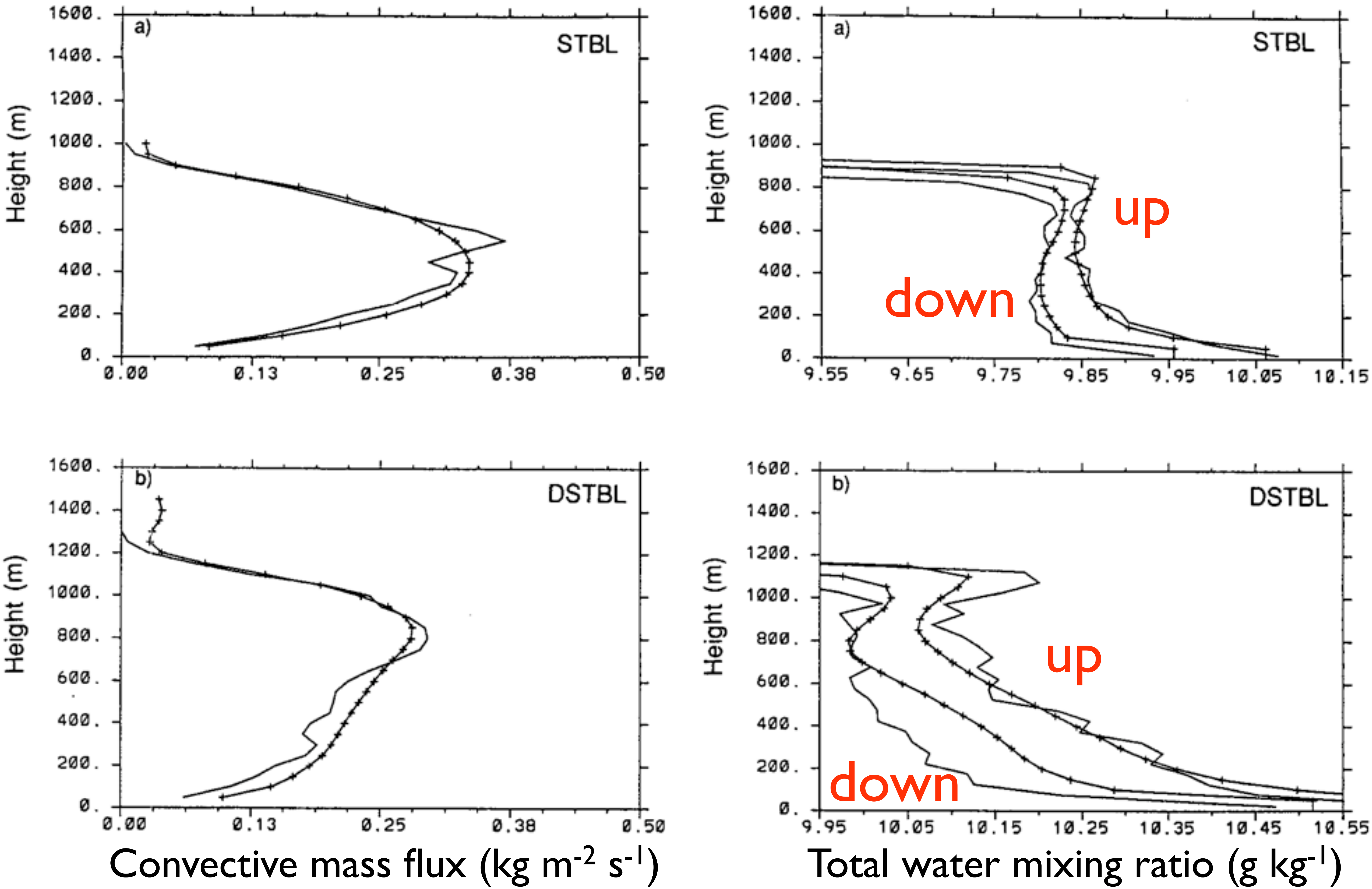
a)
STBL
b)
DSTBL
Height (m)
1600.
1400.
1200.
1000.
800.
600.
400.
200.
0.
0.00
0.13
0.25
0.38
0.50
9.55
9.65
9.75
9.85
9.95
10.05
10.15
9.95
10.05
10.15
10.25
10.35
10.45
10.55
up
down
Convective mass flux (kg m-2 s-1)
Total water mixing ratio (g kg-1)

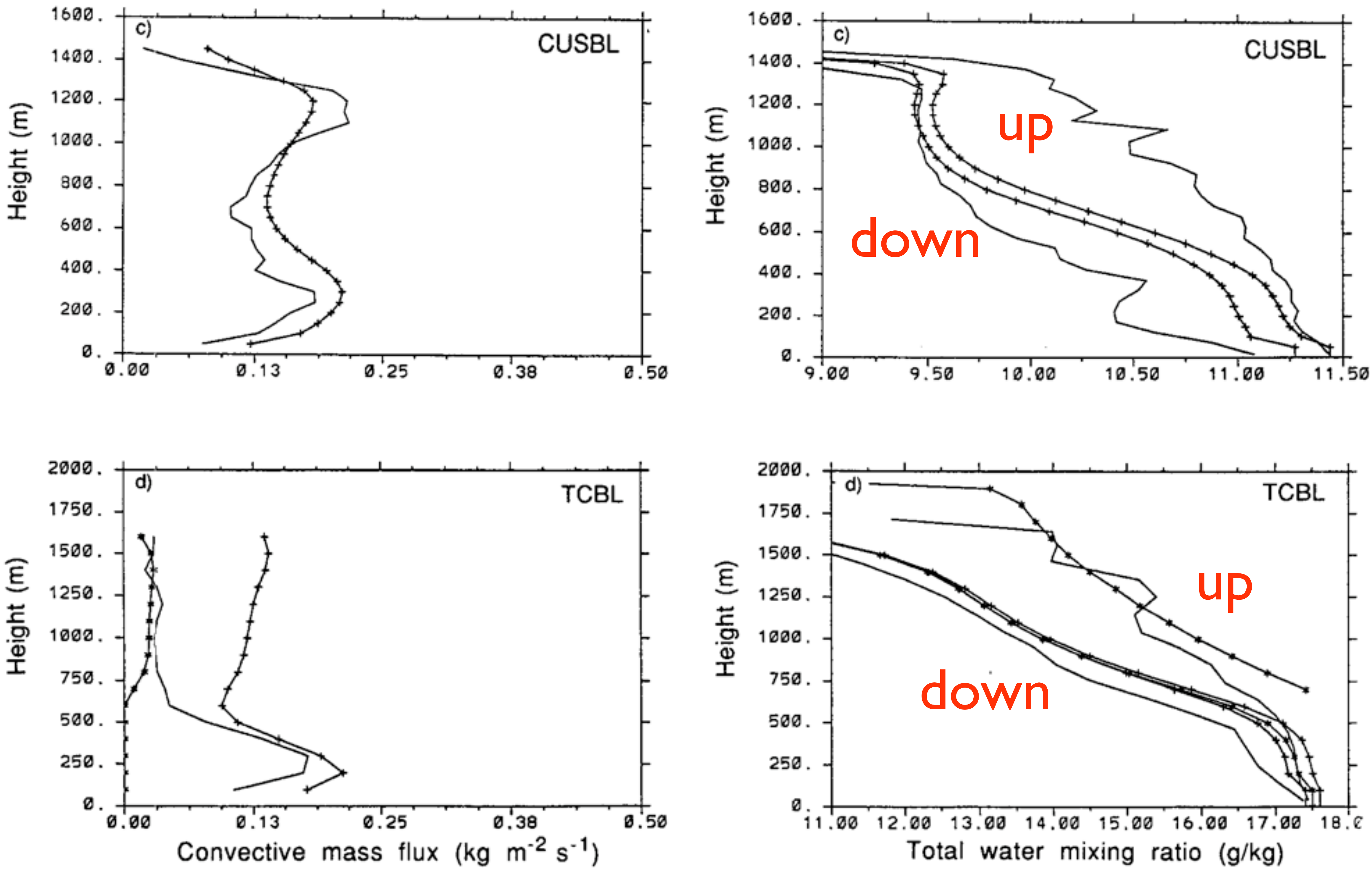

c)
CUSBL
Height (m)
up
down
d)
TCBL
Convective mass flux (kg m^{-2} s^{-1})
Total water mixing ratio (g/kg)

The following results are based on a subset of the trajectories called *penetrative* updrafts and downdrafts:

- *penetrative updrafts* start near the surface.
- *penetrative downdrafts* start near cloud top.

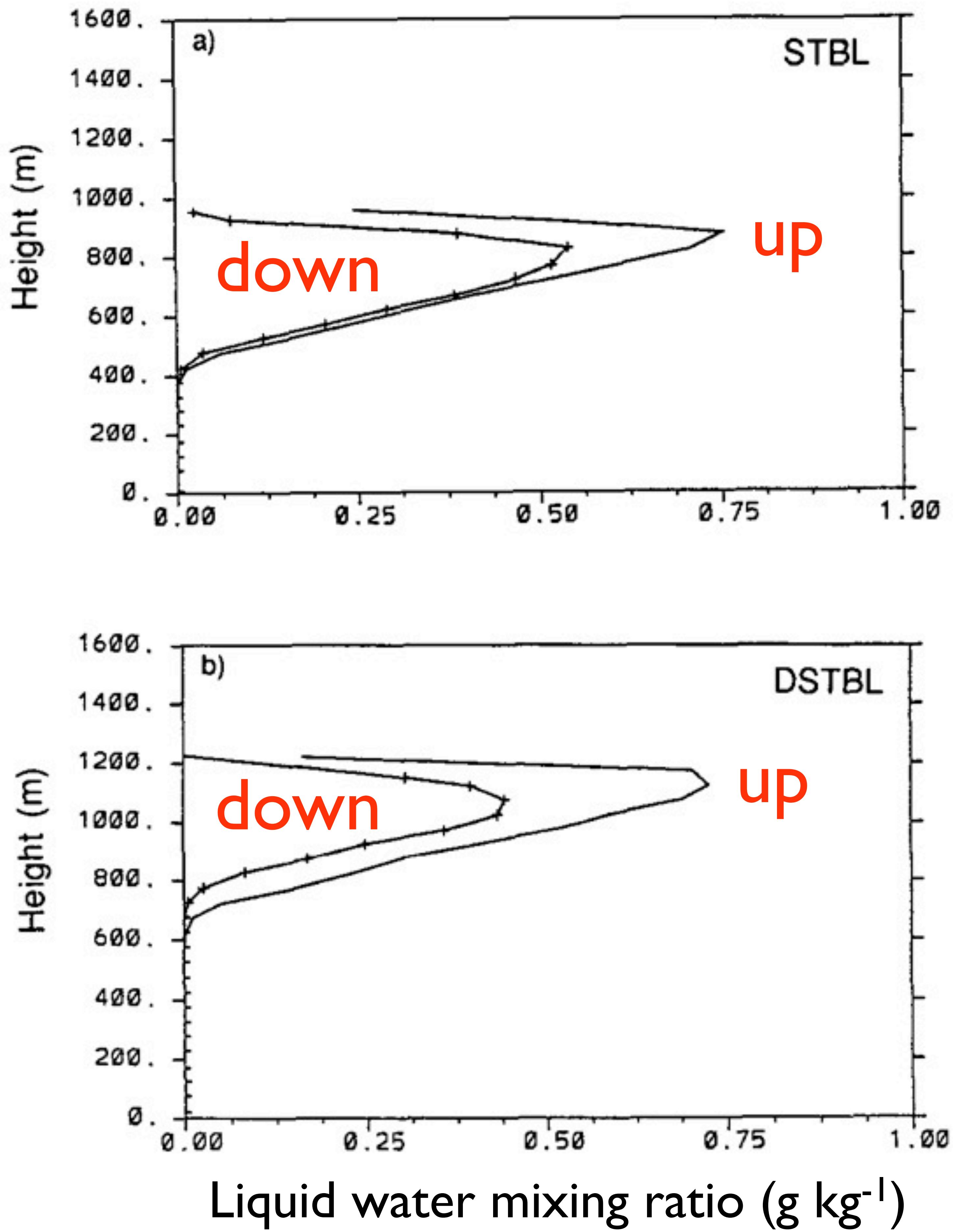
a)
STBL
down
up
Height (m)
b)
DSTBL
down
up
Height (m)
Liquid water mixing ratio (g kg-1)

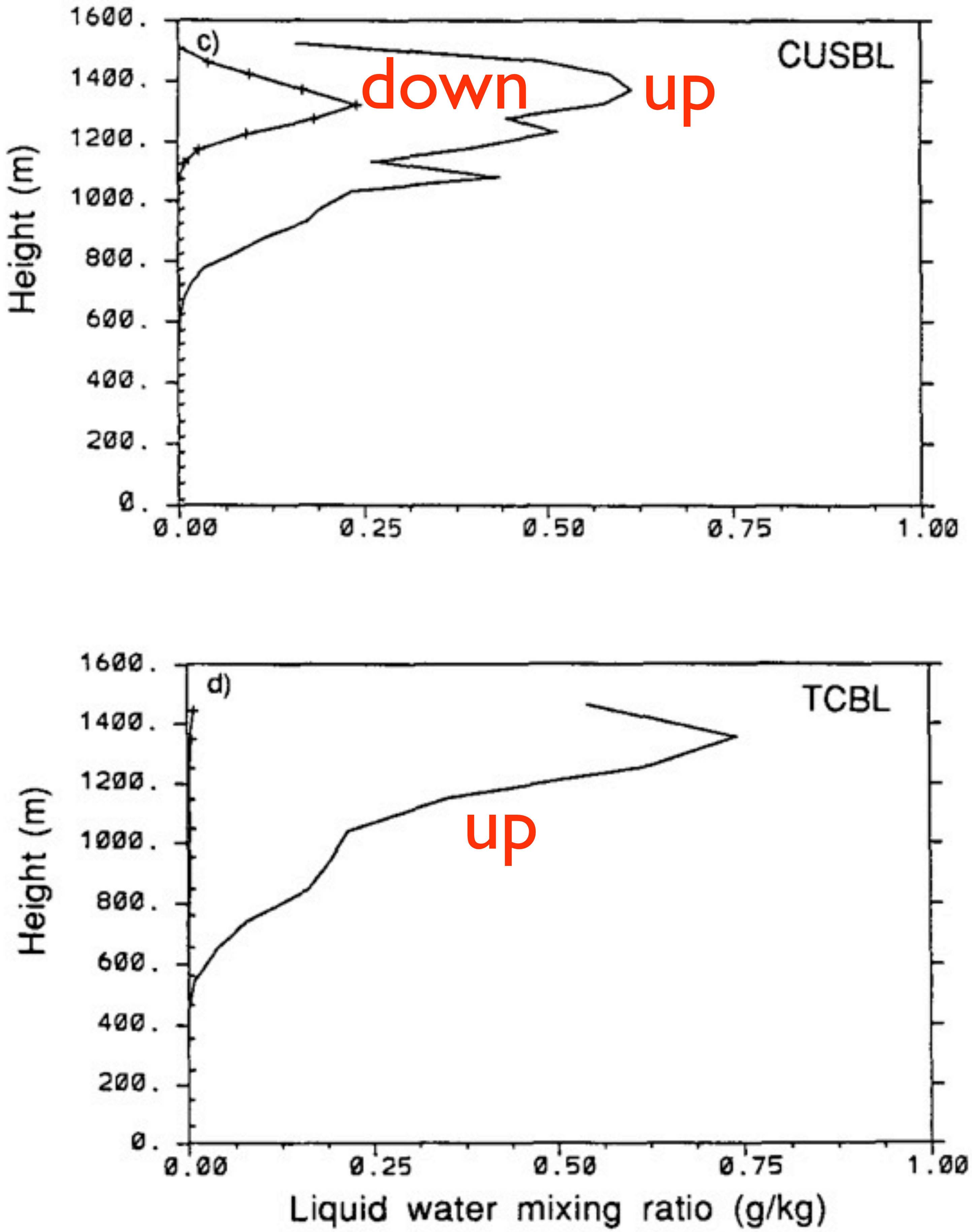

c)
CUSBL
down
up
d)
TCBL
up
Height (m)
Liquid water mixing ratio (g/kg)

b. Vertical acceleration components

A parcel's vertical acceleration is governed by

$$\frac{dw}{dt} = -\frac{\partial}{\partial z}(c_p\theta_{v0}\pi_d) + \left(B - \frac{\partial}{\partial z}(c_p\theta_{v0}(\pi_b - \pi_0))\right) + F_w, \quad \text{(C1)}$$

- dynamic p.g.f. (pressure gradient force)
- buoyancy force, including buoyancy p.g.f.
- turbulent mixing (relatively unimportant)

where B is the buoyancy:

$$B = g\left(\frac{\theta - \theta_0}{\theta_0} + 0.61(q_v - q_{v0}) - q_l\right).$$

The subscript 0 indicates a reference state variable, θ is the potential temperature, q_v is the water vapor mixing ratio, q_l is the liquid water mixing ratio, $\theta_{v0} = \theta_0(1 + 0.61q_{v0})$, and π is the Exner function:

$$\pi = \left(\frac{p}{p_{00}}\right)^{R/c_p}.$$

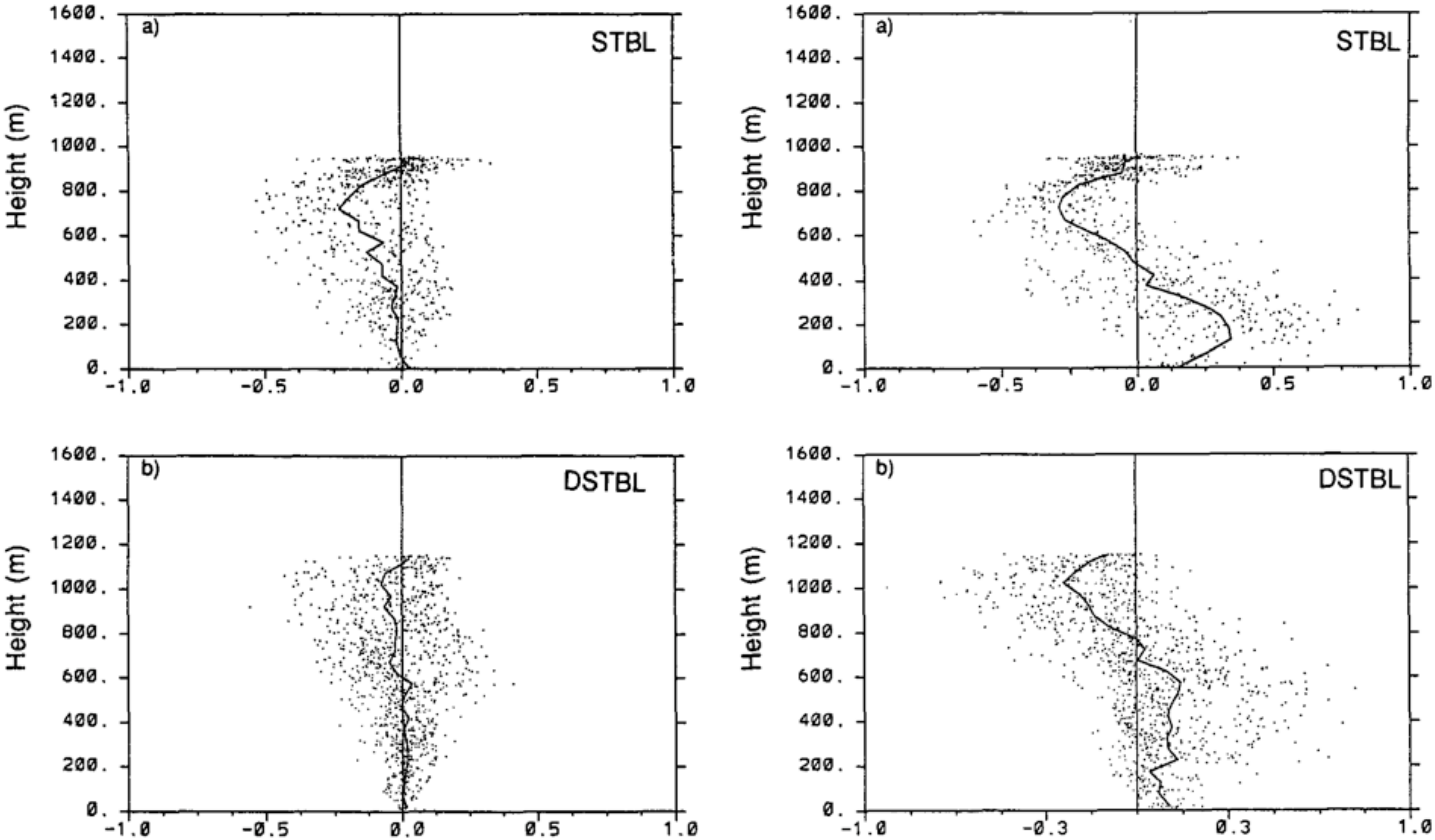

Downdraft buoyancy force
(m/s per 150 s)

Downdraft dynamic p. g. f
(m/s per 150 s)

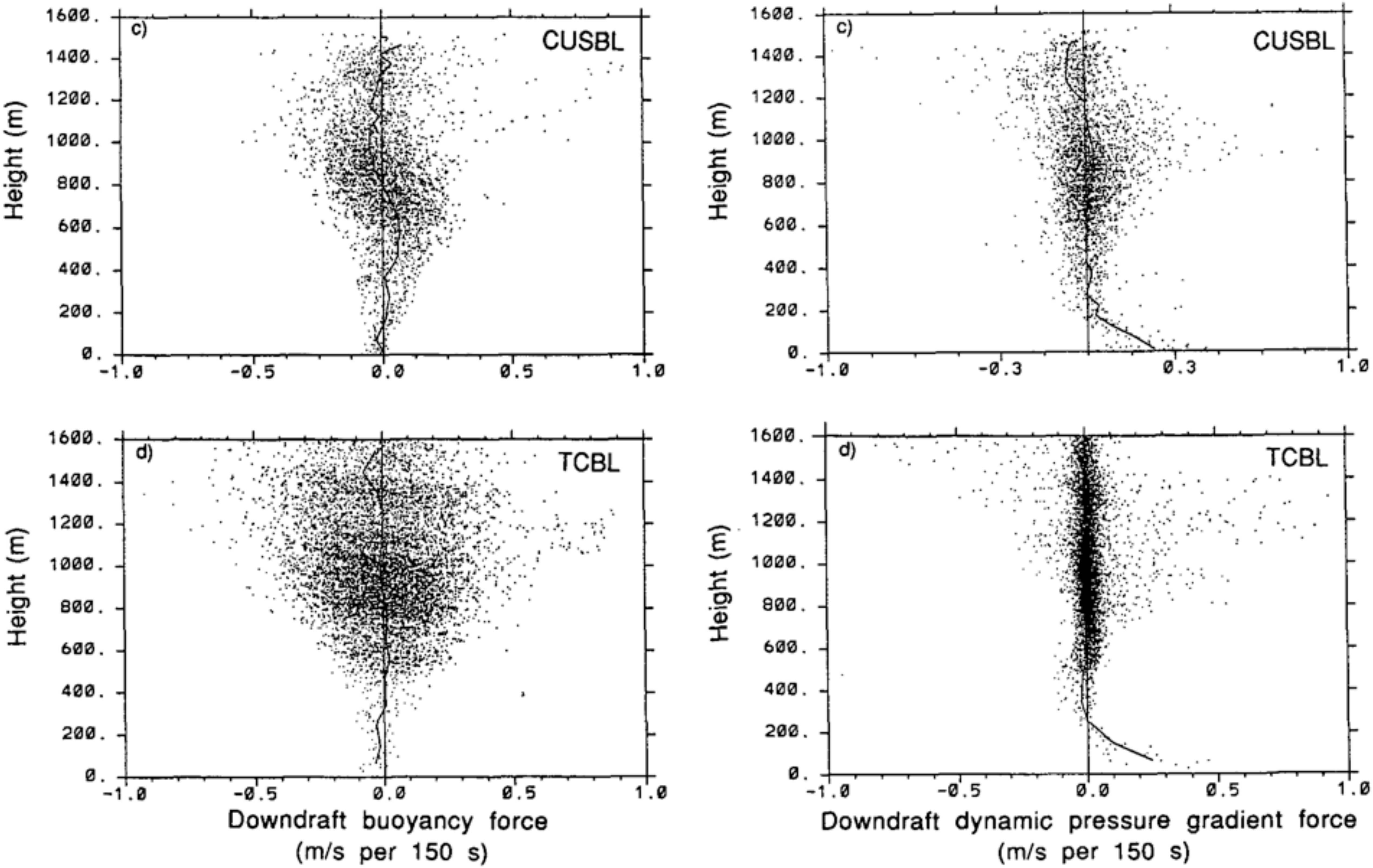
c)
CUSBL
Height (m)
1600.
1400.
1200.
1000.
800.
600.
400.
200.
0.
-1.0
-0.5
0.0
0.5
1.0
c)
CUSBL
Height (m)
-1.0
-0.3
0.3
1.0
d)
TCBL
Height (m)
-1.0
-0.5
0.0
0.5
1.0
Downdraft buoyancy force
(m/s per 150 s)
d)
TCBL
Height (m)
Downdraft dynamic pressure gradient force
(m/s per 150 s)

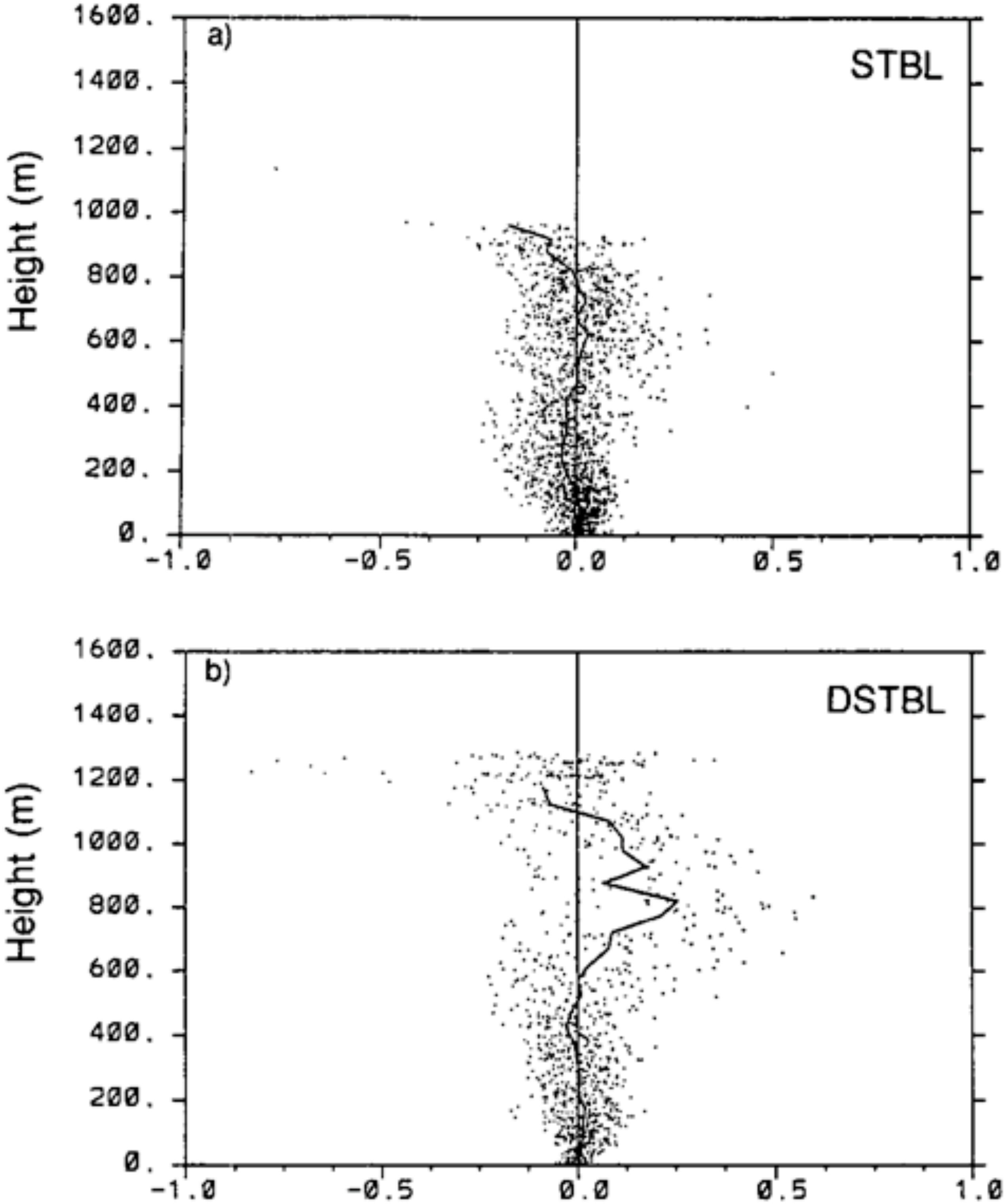

Updraft buoyancy force
(m/s per 150 s)

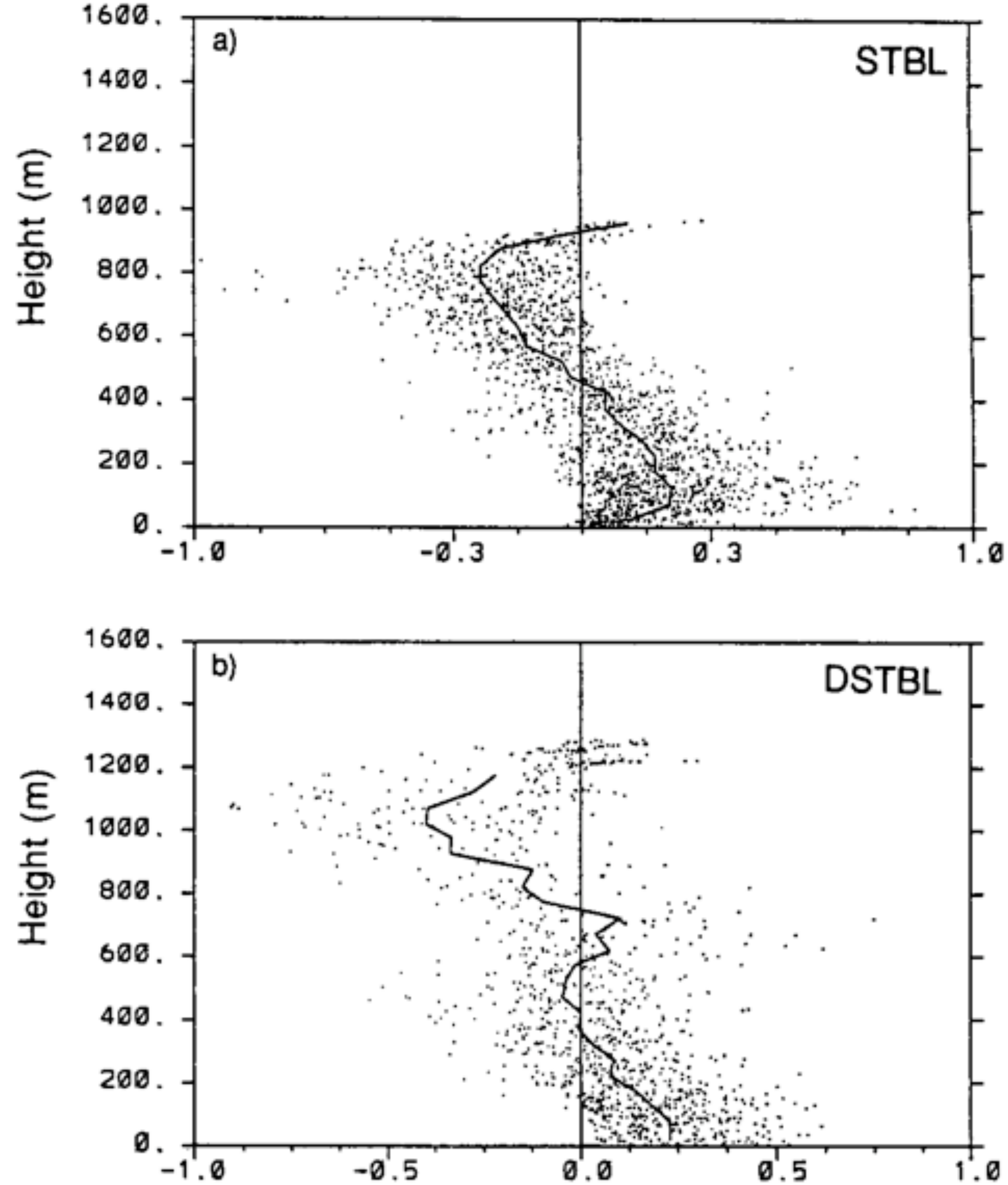

Updraft dynamic p. g. f
(m/s per 150 s)

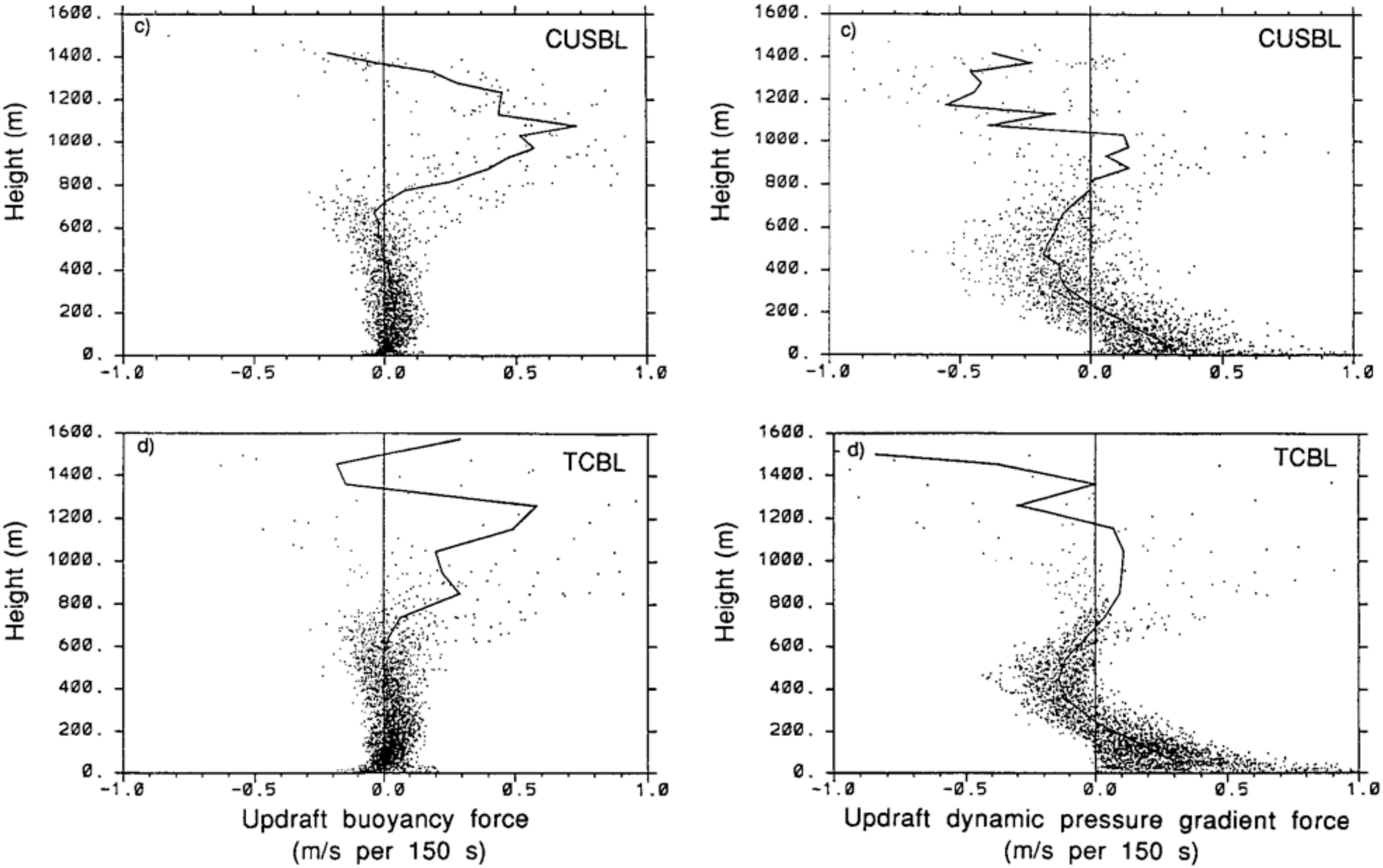
c)
CUSBL
d)
TCBL
Height (m)
Updraft buoyancy force
(m/s per 150 s)
Updraft dynamic pressure gradient force
(m/s per 150 s)

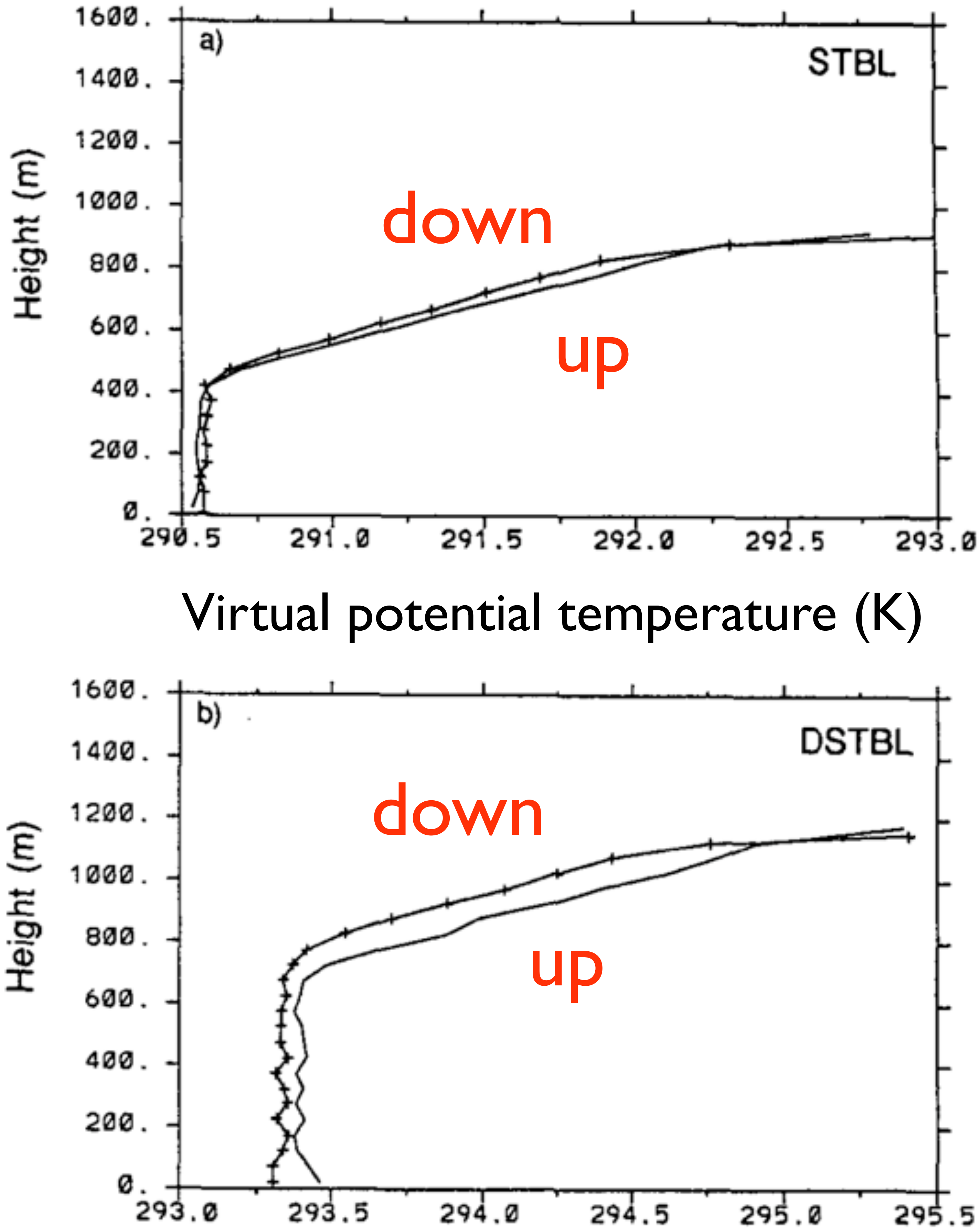

a)
STBL
down
up
Height (m)
1600.
1400.
1200.
1000.
800.
600.
400.
200.
0.
290.5
291.0
291.5
292.0
292.5
293.0
Virtual potential temperature (K)
b)
DSTBL
down
up
Height (m)
1600.
1400.
1200.
1000.
800.
600.
400.
200.
0.
293.0
293.5
294.0
294.5
295.0
295.5

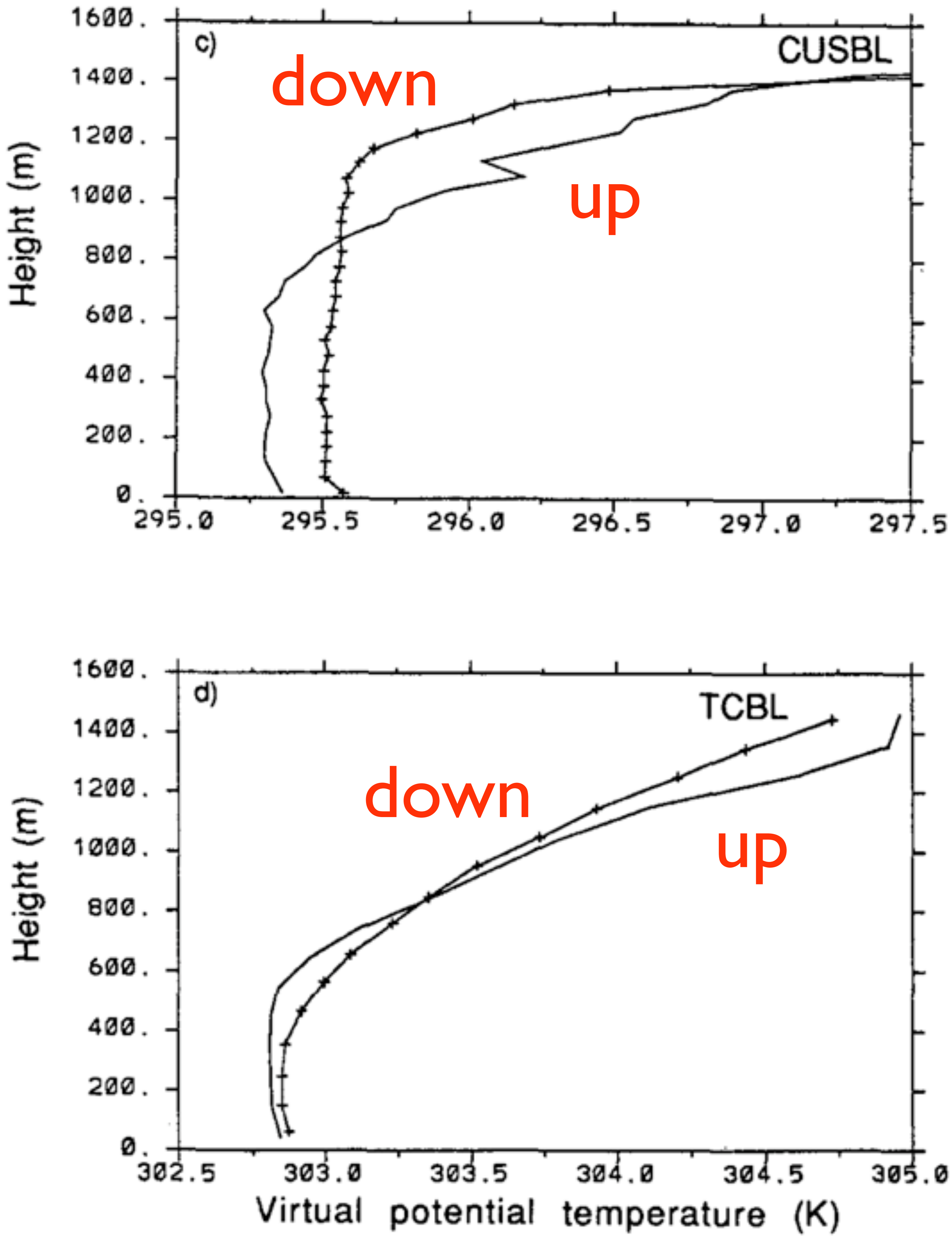

c)
CUSBL
down
up
d)
TCBL
down
up
Height (m)
Virtual potential temperature (K)

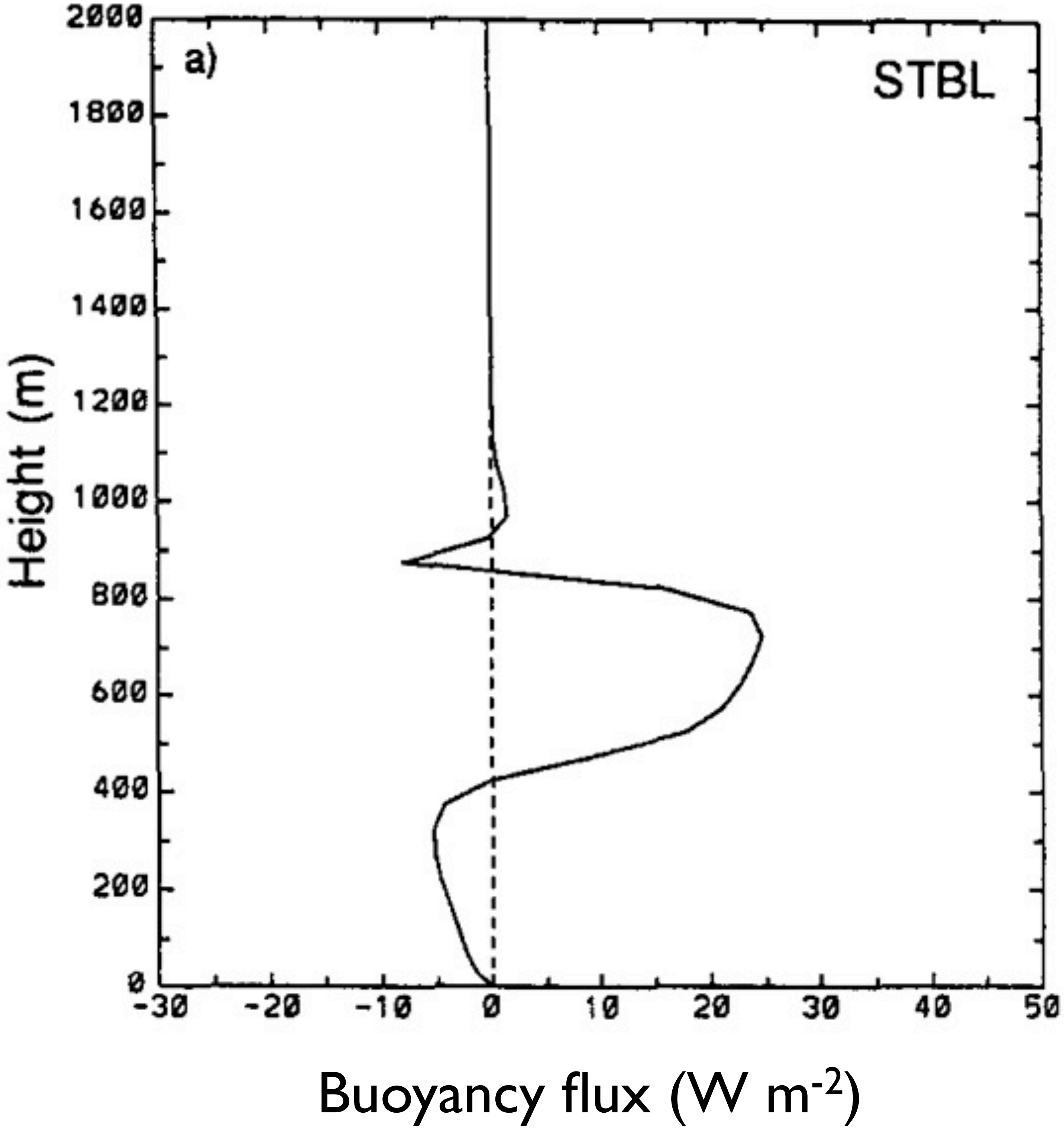

a)
STBL
Height (m)
2000
1800
1600
1400
1200
1000
800
600
400
200
0
-30
-20
-10
0
10
20
30
40
50
Buoyancy flux (W m-2)

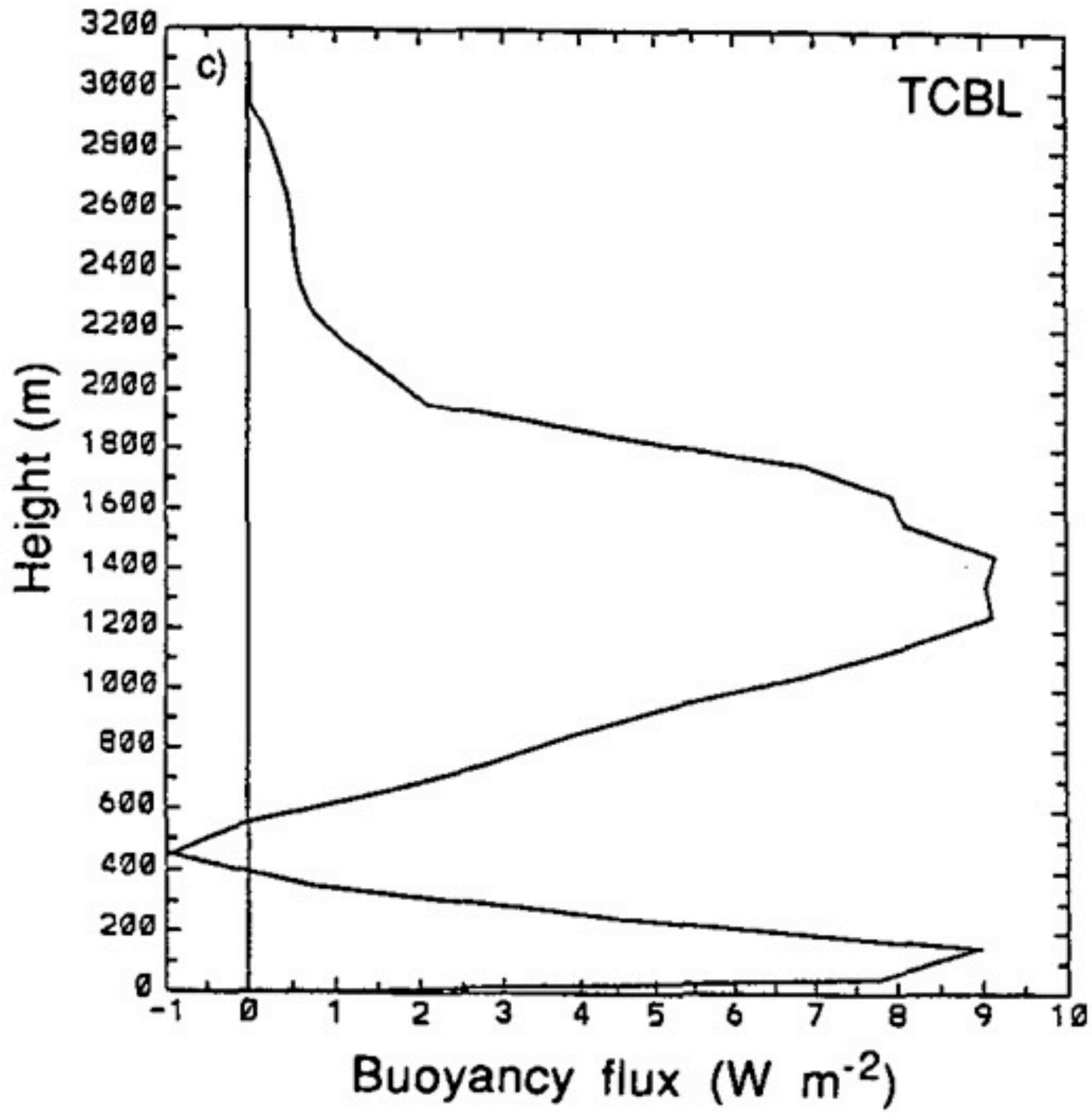
c)
TCBL
Height (m)
Buoyancy flux (W m-2)
3200
3000
2800
2600
2400
2200
2000
1800
1600
1400
1200
1000
800
600
400
200
0
-1
0
1
2
3
4
5
6
7
8
9
10

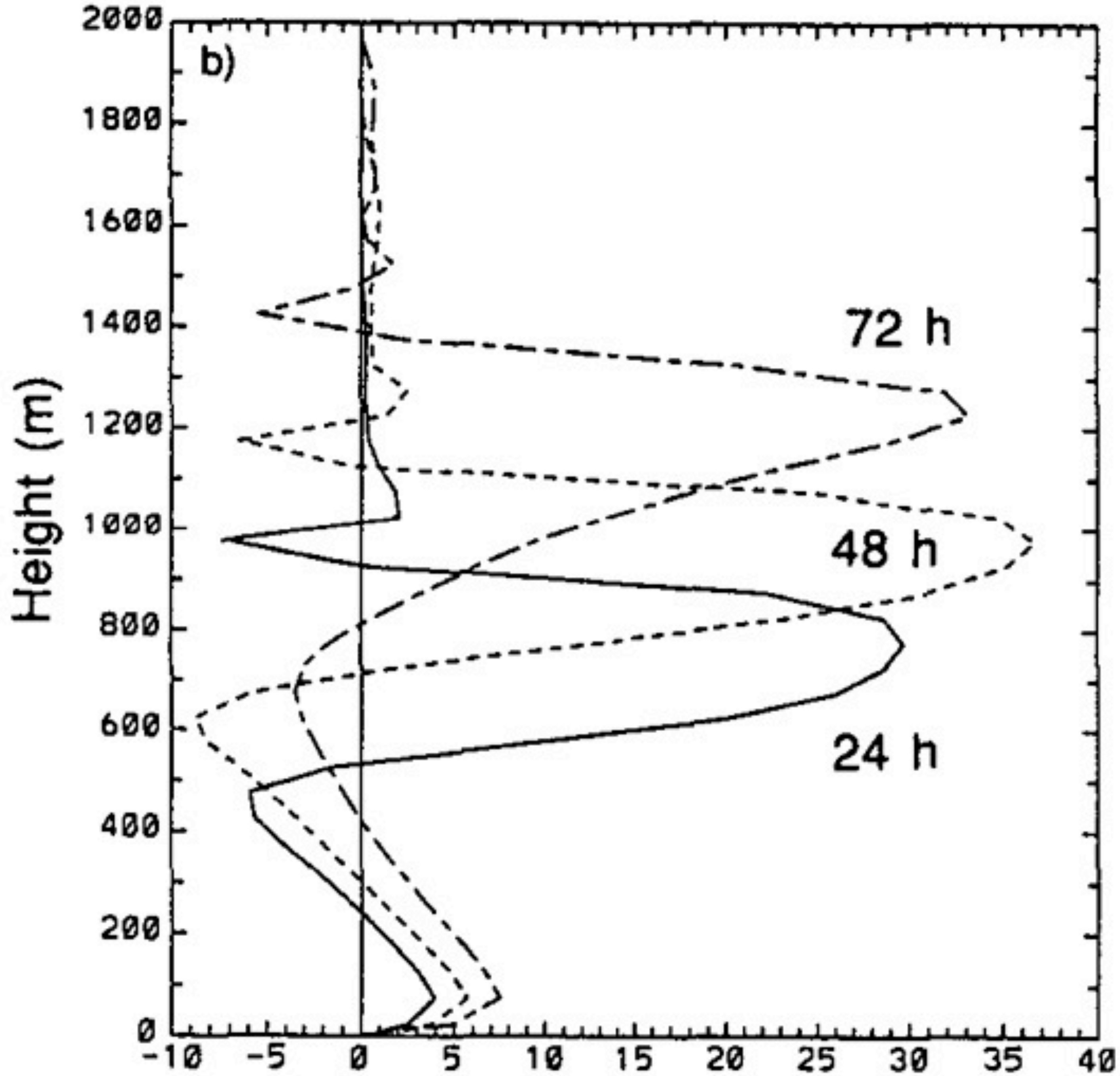

Buoyancy flux (W m^{-2})

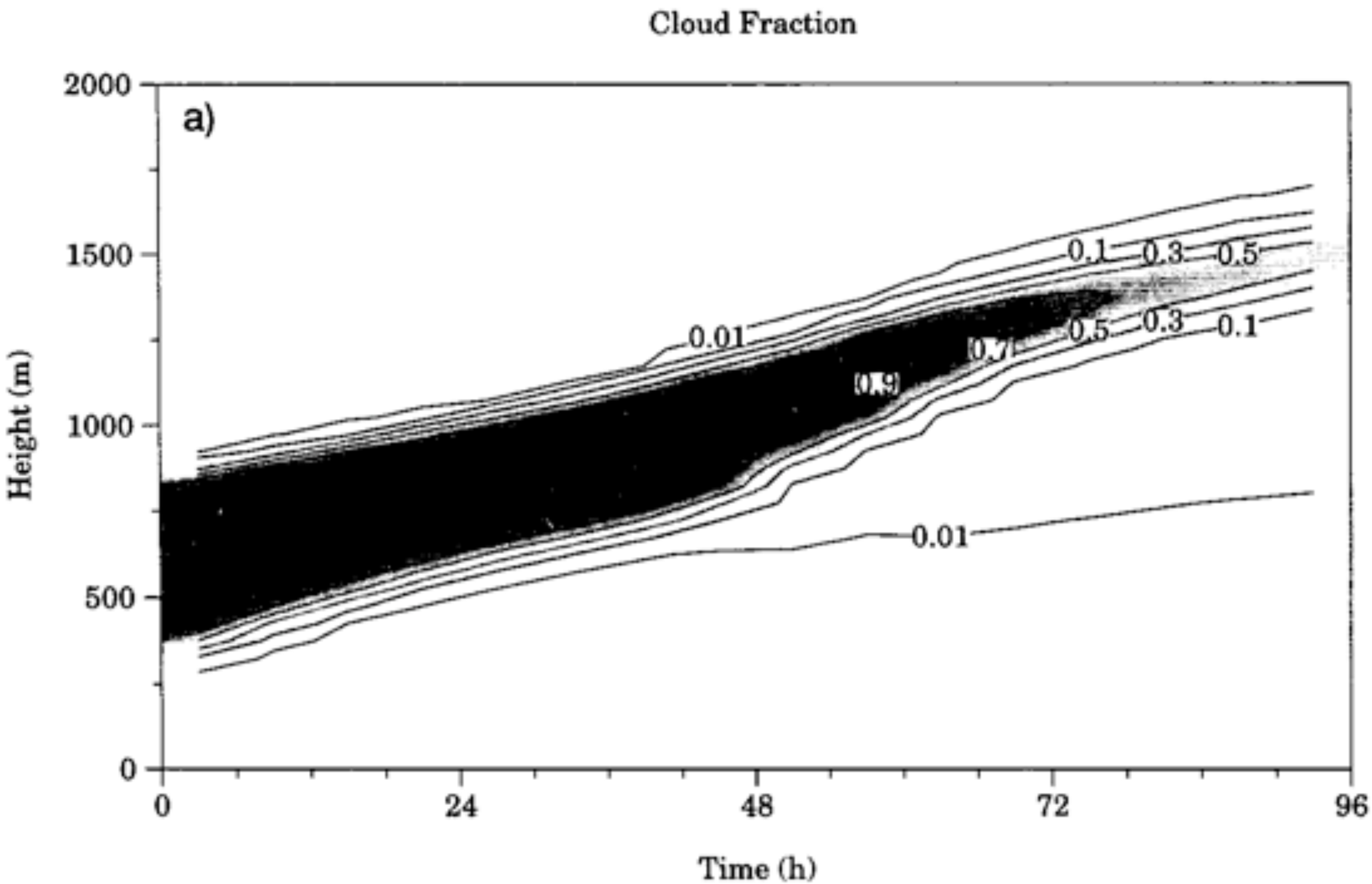
Cloud Fraction
a)
Height (m)
Time (h)
2000
1500
1000
500
0
0
24
48
72
96
0.01
0.1
0.3
0.5
0.5
0.3
0.1
0.7
0.9
0.01

Updraft buoyancy flux

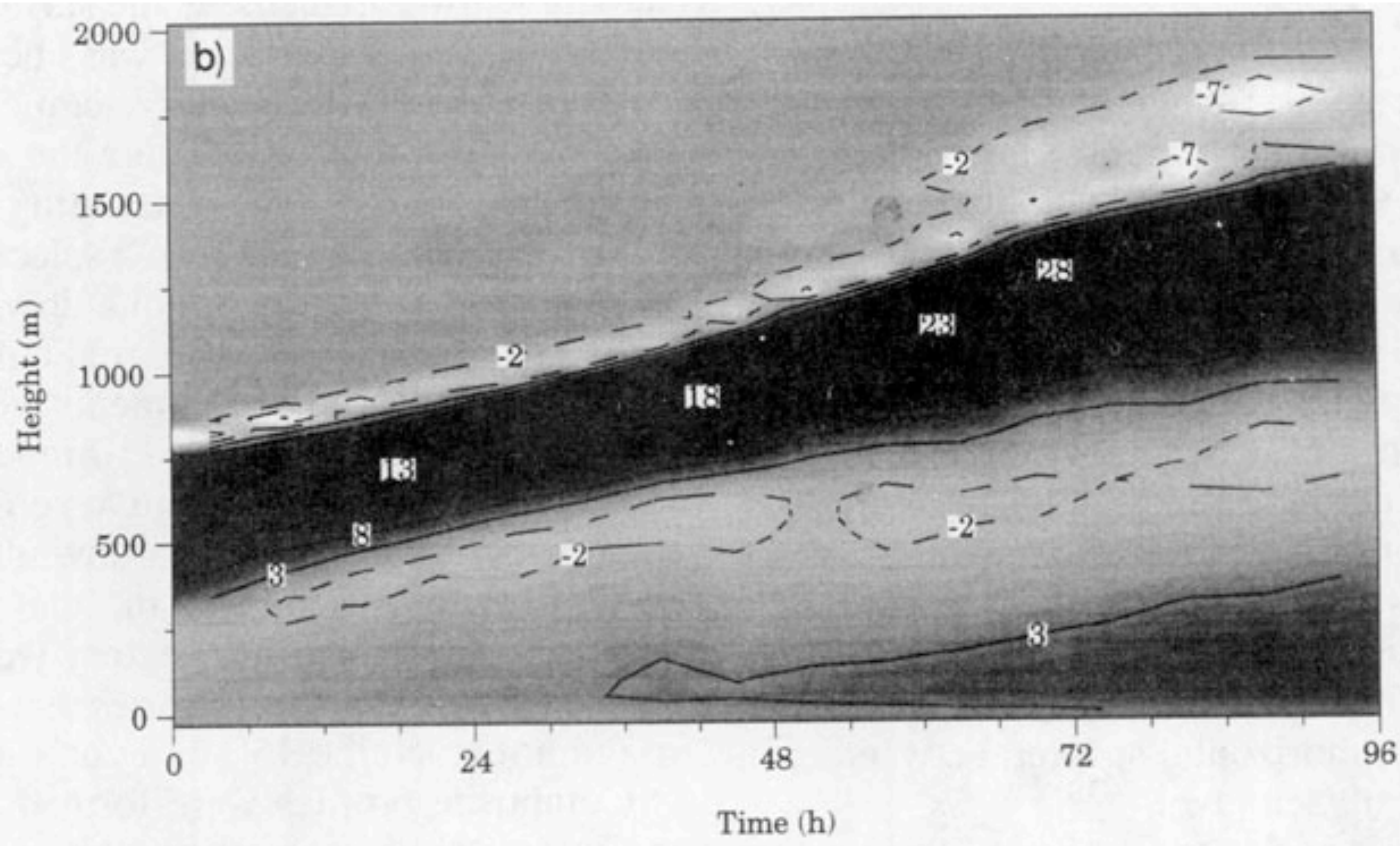

Downdraft buoyancy flux

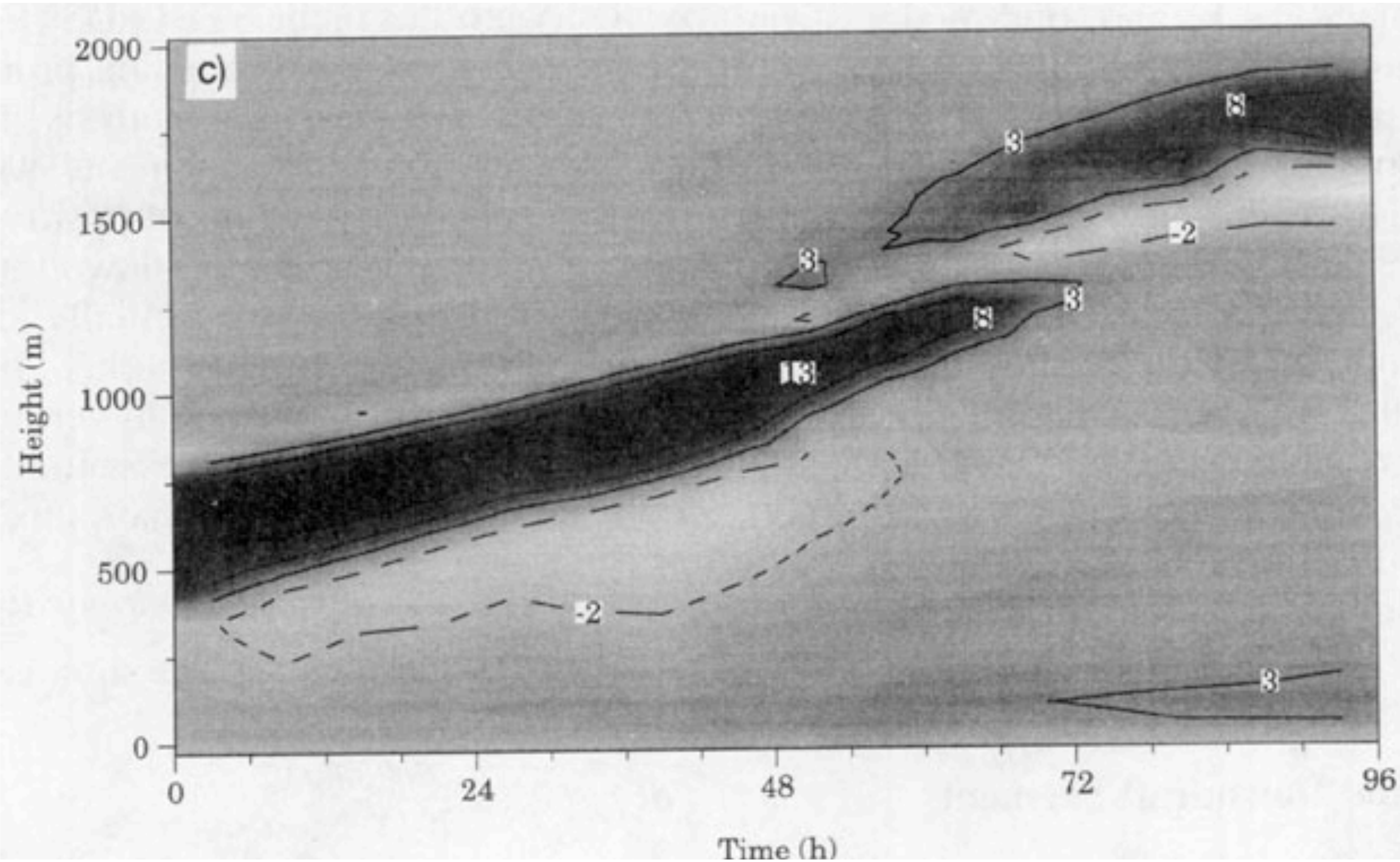

LES of Trade Cumulus

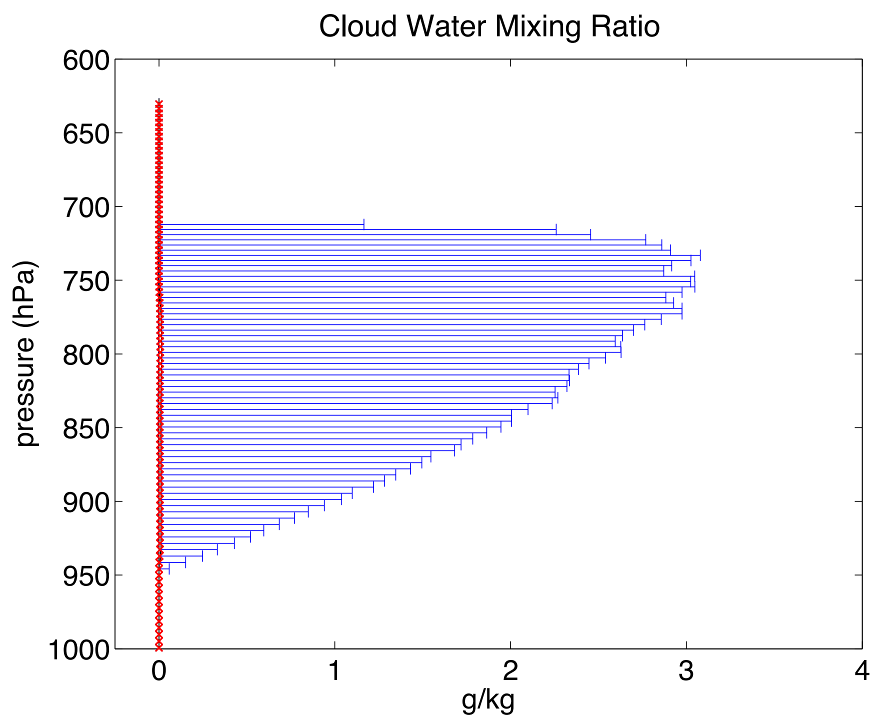

(a)

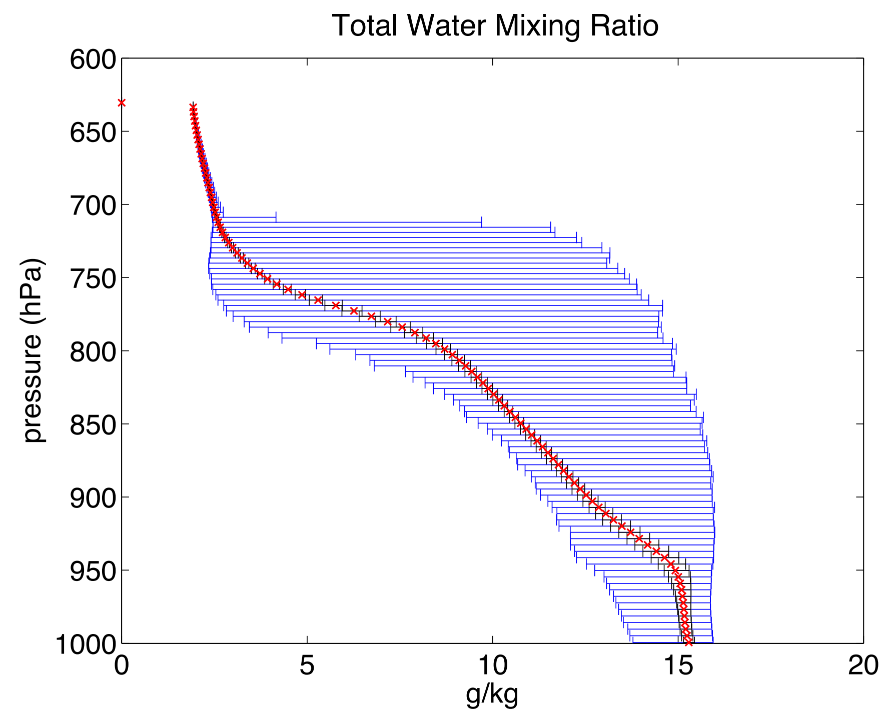

(b)

Analyses and plots by
Pete Bogenschutz

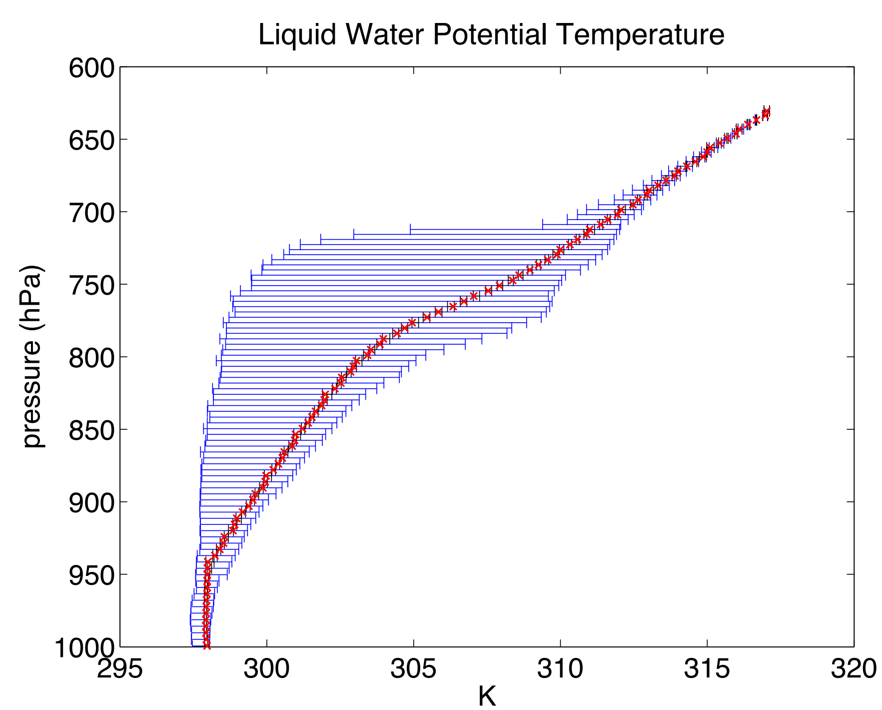

(c)

Figure 6: 100 m resolution for all points, red x denotes mean, black bars denotes 25 and 75 percent quantiles, blue bars denote minimum and maximum values.

LES of Trade Cumulus

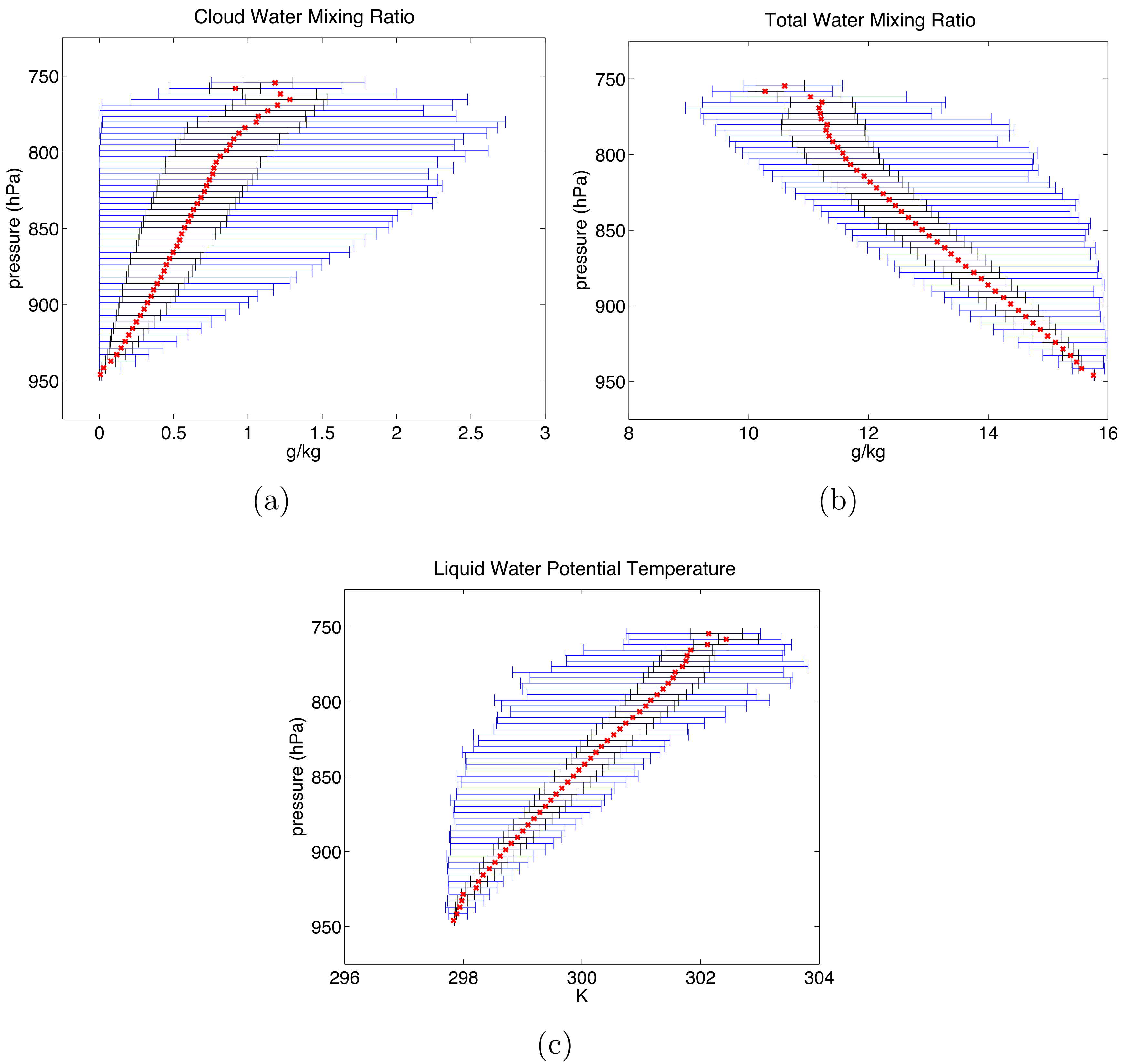

Figure 3: 100 m resolution for cloud segment points, red x denotes mean, black bars denotes 25 and 75 percent quantiles, blue bars denote minimum and maximum values.

Entraining Parcel Model of Trade Cumulus

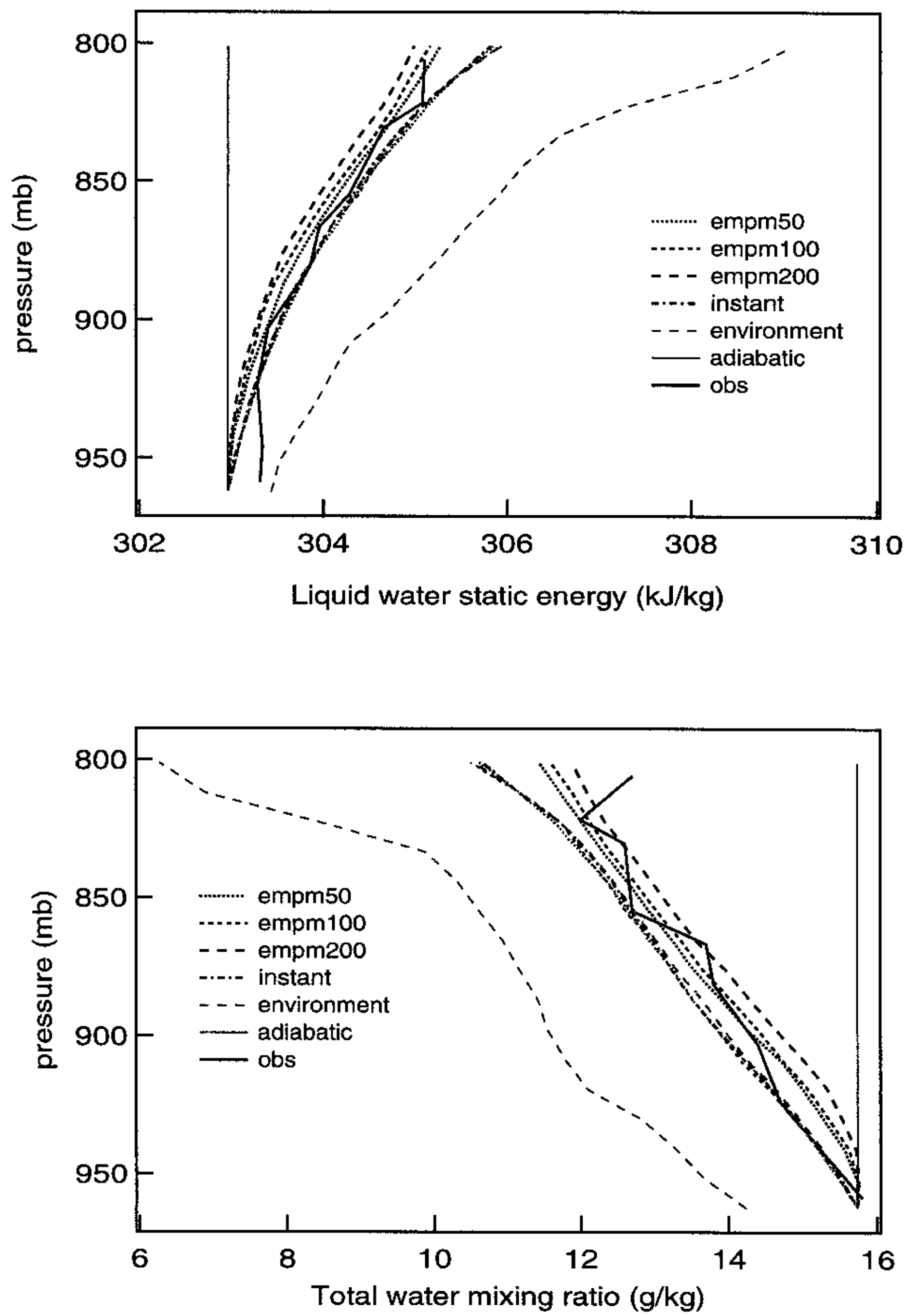

FIG. 5. Profiles of the in-cloud means of s_l and q_w obtained from observations, the instant mixing parcel model, and from the EMPM (for entrained blob sizes of 50, 100, and 200 m) using conditional sampling (black lines) and complete sampling (gray lines). For reference, the environmental and adiabatic (nonentraining) parcel model profiles are also included.

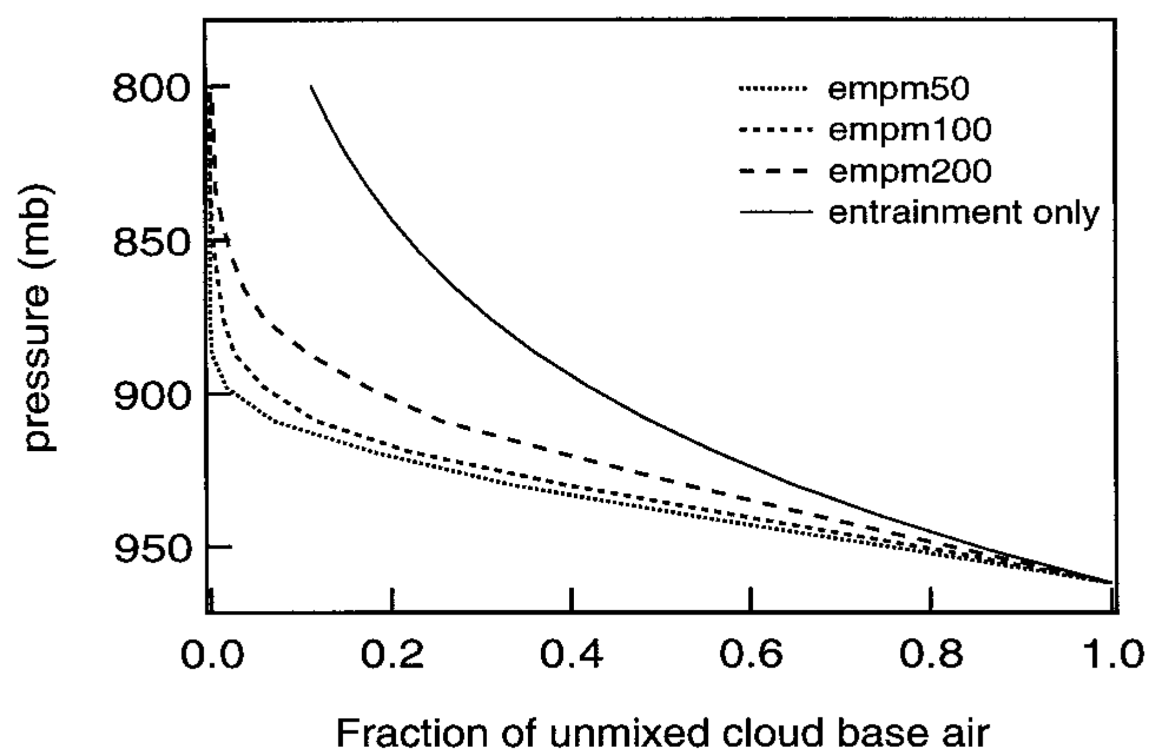

FIG. 9. Profiles of the ensemble average fraction of unmixed cloud base air from the EMPM for entrained blob sizes of 50 m, 100 m, and 200 m. The profile for entrainment with no mixing is also shown.

from Krueger et al. 1997